Aust. J. Phys., 1994, 47, 329–60

Spectroscopic and Piezospectroscopic Studies of the Energy States of Boron in Silicon

R. A. Lewis, P. Fisher and N. A. McLean

Department of Physics, University of Wollongong, Wollongong, N.S.W. 2522, Australia.

Abstract

The $p_{3/2}$ optical absorption spectrum of boron impurity in silicon has been re-examined at high resolution. The precise transition energies measured agree with energies previously reported. In addition, energies for several previously unrecognised transitions are given as well as values for the absorption strengths and line widths. The measured transition energies and absorption strengths correlate very well with several recent calculations of binding energies and oscillator strengths, respectively. This excellent agreement between experiment and theory motivates a renumbering of the spectral lines which is not expected to require future modification. High-resolution piezospectroscopy of the $p_{3/2}$ series has also been undertaken. Small stresses were used to minimise the effect of interactions and permit accurate determination of the deformation potential constants. The deformation potential constants are found to be in fair agreement with previous experimental values and good agreement with recent theory. Experimental values for several of these are given for the first time, as are isotropic deformation potential constants of several excited states relative to the ground state.

1. Introduction

For over a century, sharp lines arising from transitions of electrons between distinct energy states have been observed in the spectra, both emission and absorption, of hydrogen, the set of lines involving the state of lowest energy being known as the Lyman series. An analogous Lyman series, appearing in a solid-state analogue of hydrogen, boron-doped silicon, was observed forty years ago by Burstein *et al.* (1951). Since then numerous photoexcitation lines, associated with a range of impurities in a variety of semiconductor hosts, have been studied, the work being successively reviewed by Fisher and Ramdas (1969), Bassani *et al.* (1974), and Ramdas and Rodriguez (1981). In spite of much study, experimental interest in the excitation spectra of Si(B) continues, Fischer and Rome (1983) having reported the most comprehensive spectra to date. This continued interest derives in part from advances in experimental technique but is also spurred on by new detailed theoretical calculations of the energies of the acceptor states and the strengths of the transitions, as demonstrated in the recent work of Pajot *et al.* (1992).

The basic theory of shallow acceptor states in semiconductors, the effective mass approximation, is a generalisation of the solution of the hydrogen Schrödinger equation (Kittel and Mitchell 1954; Luttinger and Kohn 1955). The effective mass approximation was rendered amenable to calculation by separating the Hamiltonian into a dominant spherical term (Baldereschi and Lipari 1973) and

0004-9506/94/030329$05.00

a subsidiary cubic term (Baldereschi and Lipari 1974). Treating the cubic term as a perturbation, unfortunately, is invalid for Si, where it is large; moreover this method is independent of the chemical identity of the acceptor, so is not well suited to Si(B). The calculations have been made apposite to Si(B) by further refinement of the spherical model by introduction of the spin–orbit split-off valence band, a dielectric screening function (Baldereschi and Lipari 1976; Lipari and Baldereschi 1978), a semi-empirical short-range species-dependent correction term (Lipari *et al.* 1980) and valence-band warping (Binggeli and Baldereschi 1988). The most recent calculations have yielded line strengths in addition to energies and symmetries. Starting from the complete Hamiltonian and including the split-off band and a dielectric screening function, Buczko and Bassani (1988) have calculated line positions and strengths for the group III acceptors in Si. Beinikhes *et al.* (1990) also took as their starting point the complete Hamiltonian but used a nonvariational calculation to give the positions and intensities of the Si(B), among other, states. This approach follows similar work for acceptors in Ge (Kogan and Polupanov 1978) and donors in Ge and Si (Beinikhes *et al.* 1985; Beinikhes and Kogan 1988).

Theoretical studies have also been made on the effect of external fields on the energy states. In a magnetic field the hydrogen atom displays a much richer spectrum as a consequence of the field bifurcating the energy states. This, the Zeeman effect, also appears in the hydrogen atom's solid-state counterparts. Unique to the solid state is the splitting of states due to another type of external perturbation—applied uniaxial stress—the piezospectroscopic effect. [Further, the concurrent application of a magnetic and an elastic field, known as piezo-Zeeman spectroscopy, the theory of which was developed by Bir *et al.* (1963; see also Bir and Pikus 1974) using perturbation methods, supplanted now by the exact theory of Duff (Duff *et al.* 1988; Duff 1993), has been exploited by Freeth *et al.* (1986, 1987) to interpret the Ge(III) spectra.] Piezospectroscopy of acceptors in Si, including Si(B), was systematically undertaken by Onton *et al.* (1967) who, on the basis of the polarisation features of spectra from samples under stress applied in simple crystallographic directions, were able to deduce the symmetries of the ground and several excited states. This work was extended by Chandrasekhar *et al.* (1973) who applied stresses of known magnitudes and were thus able to measure the parameters which characterise the stress splittings, the deformation potential constants, for the ground and the first two excited states of boron, as well as for states of other acceptors, in silicon. Piezospectroscopic measurements of Si(B) at high stress have been reported by Cooke *et al.* (1978). In passing it might be mentioned that Zeeman spectroscopy of Si(B) has been undertaken by Merlet *et al.* (1975), however, piezo-Zeeman spectroscopic results for Si(B) have not been reported.

The quantitative theory of the piezospectroscopic effect is a natural extension of the effective mass approximation. The most recent calculations are those of Buczko (1987). These follow on from analyses of the effect of uniaxial stress on the acceptor ground states in Ge (Buczko *et al.* 1980), Si (Chroboczek *et al.* 1984) and both Ge and Si (Buczko and Chroboczek 1984).

The present paper reports an experimental investigation, particularly directed to the little-studied higher energy states, of the spectra and piezospectra of Si(B), and compares the results with the latest theoretical analyses. Experimental values

of the positions, strengths and widths of a large number of lines in the unperturbed spectrum are given as well as an estimation of the ground state binding energy. The symmetries of many states are deduced by the stress behaviour of the spectral components of the parent lines, confirming and greatly extending previously published experimental work and generally confirming theoretical predictions. Deformation potential constants have been determined for many more states than previous experiments have allowed, the present results on occasion differing from the earlier work, but being in good agreement with the theory. A brief account of some of these findings has appeared previously in Lewis *et al.* (1988). In some instances the present results differ slightly from the latter due to recalibration of the spectrometer and other minor corrections.

2. Experimental Procedure

Six samples of dimensions in the ranges 4 to 6 mm wide, 1 to 4 mm thick and 15 to 22 mm long were cut from the same Si(B) ingot of nominally 20 Ω cm room-temperature resistivity, three with the long axis along which force was applied in a ⟨111⟩ direction, two in a ⟨100⟩ direction and one in a ⟨110⟩ direction. The samples were cut with a wire saw (Model Number 850, South Bay Technology, California), crystallographically aligned by the optical method of Hancock and Edelman (1956) using a laser source, wedged slightly to minimise optical interference between the front and back faces, and mechanically polished to a 6 μm finish.

The cross-sectional area of each sample, required to calculate the stress from the applied force, was measured in two ways: directly, by multiplying the width and thickness, and indirectly, by dividing the mass of the sample by its length and by the density of Si, the value of density used being that of Smakula and Sils (1955). Salib *et al.* (1985) found the difference between these two methods for Ge samples was always less than 0·75%. For the present samples the direct method always gave a *greater* value, by 0·57% to 1·14%, an amount which generally increased with sample size. No source of error could be found in the measurement process itself and in reviewing the detailed data of Salib (1982) the direct measurement was seen to give in every instance a greater value for the area than the indirect method. The difference is attributed to rounding of the sample edges in polishing and is consistent with an average radius of curvature of 0·32±0·03 mm.

The samples were mounted in a cryostat of the type, and using the techniques, described by Salib (1982) and were cooled using liquid He; this cryostat and these techniques are modifications of those described by Tekippe *et al.* (1972). The temperature of the sample, thermally connected to the He bath by a cold finger, was not measured directly, but is believed to be in the range 5 to 10 K. Uniaxial compression was applied in a simple fashion by resting calibrated lead or brass masses on a push rod which transmitted the weight force to the sample. This procedure gives the impressed force accurately and directly, and permits the application of small, well-defined, stable forces. In converting the applied force to stress, the cross-sectional area as determined by the indirect method was used. The correction in sample area due to thermal contraction of Si is negligible (Swenson 1983) and so was not applied. The local value of gravitational acceleration given by Wellman *et al.* (1985) was used.

The source of radiation was a globar, dissipating about 220 W, and the radiation was modulated at 410 Hz by a mechanical chopper before being fed by entrance optics into a single-beam double-grating monochromator (Model Number 1402, Spex Industries, Metuchen, New Jersey) fitted with gratings blazed at $31{\cdot}0\pm0{\cdot}3\ \mu$m (nominally 30 μm) and flushed with dry air to reduce the partial pressure of water vapour. Polarisation was accomplished by a wire-grid polariser on a polyethylene substrate (Perkin–Elmer Corp., Main Avenue, Norwalk, Connecticut). The detector was a germanium bolometer (Unit #804, Infrared Laboratories, Inc., Tucson, Arizona) furnished with a wedged sapphire filter, cooled by liquid helium, the enclosure of which was usually evacuated to lower the temperature and thus improve the signal-to-noise ratio.

Data were collected using a lock-in amplifier (Model Number HR8, Princeton Applied Research Corporation, Princeton, New Jersey), digitised by a DVM (Model Number AD-2008, Analog Devices, Norwood, Massachusetts) and stored in an Apple II computer. They were subsequently transferred to a Macintosh SE computer for analysis and plotting.

In converting the data from transmission to absorption, the refractive index of Si given by Loewenstein *et al.* (1973) was used, as were the Si elastic compliance coefficients of Hall (1967) in calculating the deformation potential constants.

3. Theory

The theoretical approaches which yield energies and oscillator strengths of states associated with B in Si were briefly described in Section 1. The results

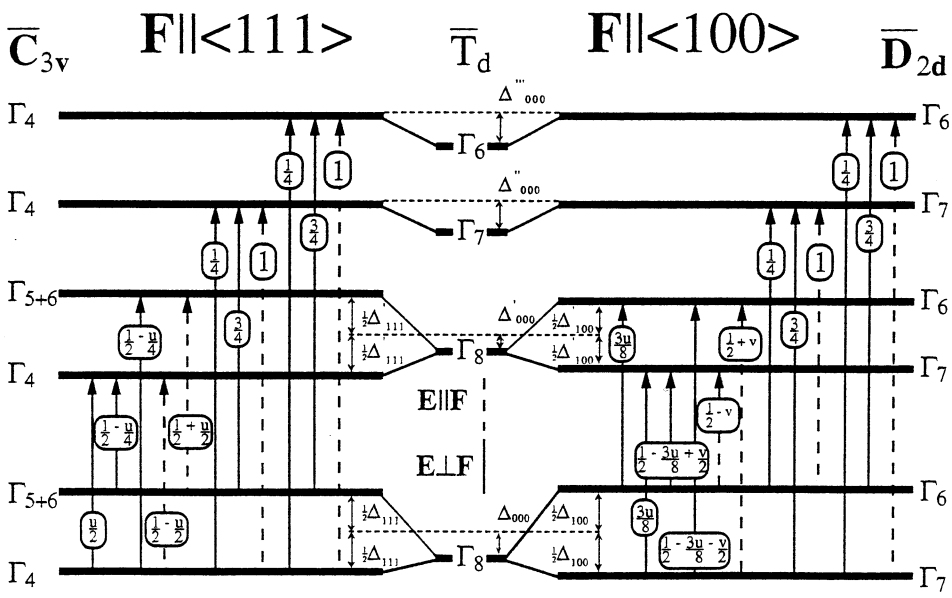

Fig. 1. Allowed transitions and intensities from a Γ_8 ground state to Γ_8, Γ_7 and Γ_6 excited states of the double group $\overline{T}_d$ for an applied force in the $\langle 111\rangle$ or $\langle 100\rangle$ directions. The parameters u and v determine the relative intensities of the components arising from the Γ_8 manifold of the ground state and that of a Γ_8 excited state. The values of u and v range from 0 to 1, and from $-\frac{1}{2}$ to $\frac{1}{2}$, respectively (see Rodriguez *et al.* 1972).

of recent calculations by Buczko and Bassani (1989), Binggeli and Baldereschi (1989), and Beinikhes *et al.* (1990) will be presented as appropriate in Section 4. For particulars of the method followed in each instance, the reader is referred to Buczko and Bassani (1988), Binggeli and Baldereschi (1988) and Beinikhes *et al.* (1990). Each of these treatments also classifies the various states according to their symmetry.

In order to demonstrate how the piezospectra can reveal the symmetry of the hole states, it is convenient to recapitulate the way the pertinent states split under stress, and the optical selection rules governing transitions between the substates for $\boldsymbol{E} \parallel \boldsymbol{F}(E_{\parallel})$ and $\boldsymbol{E} \perp \boldsymbol{F}(E_{\perp})$, where $\boldsymbol{E}$ is the electric field of the radiation and $\boldsymbol{F}$ is the applied force. These are presented in Fig. 1, which also gives the relative intensities of the allowed transitions from the ground state manifold to each of the three types of final state manifolds, in terms of the parameters u and v, as deduced by Rodriguez *et al.* (1972) from symmetry arguments, assuming no interaction between any of the manifolds.

Theoretical values of the deformation potential constants have been given by Buczko (1987). To determine the deformation potential constants from the experimental energies of the components produced by the application of uniaxial stress, the results of the theory following Pikus and Bir (1959) and Rodriguez *et al.* (1972) are set out below.

(3*a*) *Applied Force in a* ⟨111⟩ *Direction*

For a tetrahedral semiconductor of elastic compliance coefficients s_{jk} under a force applied parallel to ⟨111⟩, the hole energy for a Γ_8 state, relative to an arbitrary zero of energy, is given by

$$E_i = \epsilon_i + a_i(s_{11} + 2s_{12})T \pm (d_i/2\sqrt{3})s_{44}T\,, \tag{1}$$

where T is the stress (negative for compressive forces), a and d are the hydrostatic and one of the deformation potential constants, respectively, ϵ_i is the unperturbed energy and the index i distinguishes states. The ground state of acceptors in silicon ($i = 0$) is known to be a Γ_8 state (Onton *et al.* 1967) and so follows this equation. Under the relatively small stresses used in the present experiments, the stress splitting, $\Delta_{111}^{(i)} = (d_i/\sqrt{3})s_{44}T$, for any Γ_8 excited state i, is much less than the separation in energy of the ground and excited state, $h\nu_i = \epsilon_i - \epsilon_0$. Denoting $\Delta_{000}^{(i)} = a_i(s_{11} + 2s_{12})T$, the energies of the four possible transitions between the stress-induced substates of the ground and excited states are, as may be corroborated from Fig. 1,

$$E_{++} = h\nu_i + \Delta_{000}^{(i)} - \Delta_{000}^{(0)} + \tfrac{1}{2}\Delta_{111}^{(i)} + \tfrac{1}{2}\Delta_{111}^{(0)}\,, \tag{2}$$

$$E_{+-} = h\nu_i + \Delta_{000}^{(i)} - \Delta_{000}^{(0)} + \tfrac{1}{2}\Delta_{111}^{(i)} - \tfrac{1}{2}\Delta_{111}^{(0)}\,, \tag{3}$$

$$E_{-+} = h\nu_i + \Delta_{000}^{(i)} - \Delta_{000}^{(0)} - \tfrac{1}{2}\Delta_{111}^{(i)} + \tfrac{1}{2}\Delta_{111}^{(0)}\,, \tag{4}$$

$$E_{--} = h\nu_i + \Delta_{000}^{(i)} - \Delta_{000}^{(0)} - \tfrac{1}{2}\Delta_{111}^{(i)} - \tfrac{1}{2}\Delta_{111}^{(0)}\,. \tag{5}$$

The subscripts on E correspond to the last two signs on the right-hand side of the equation. The four transitions, when ordered according to increasing energy, are normally labelled $i.1$, $i.2$, $i.3$ and $i.4$. The deformation potential constant of the ground state, d_0, is obtained by subtracting equation (5) from (4) or equation (3) from (2), giving

$$d_0 = \frac{\sqrt{3}}{s_{44}T}(E_{-+} - E_{--}) = \frac{\sqrt{3}}{s_{44}T}(E_{++} - E_{+-}). \tag{6}$$

In a similar manner, the deformation potential constant of the excited state, d_i, is obtained by subtracting equation (5) from (3) or equation (4) from (2),

$$d_i = \frac{\sqrt{3}}{s_{44}T}(E_{+-} - E_{--}) = \frac{\sqrt{3}}{s_{44}T}(E_{++} - E_{-+}). \tag{7}$$

While a_0 and a_i are not attaintable directly, their difference is, either by adding equations (2) and (5) or by adding (3) and (4):

$$a_i - a_0 = \frac{E_{++} - E_{--} - 2h\nu_i}{2(s_{11} + 2s_{12})T} = \frac{E_{+-} + E_{-+} - 2h\nu_i}{2(s_{11} + 2s_{12})T}. \tag{8}$$

If the excited state has Γ_6 or Γ_7 symmetry, it is not split by uniaxial stress but merely undergoes a hydrostatic shift. In this case

$$E_i = \epsilon_i + a_i(s_{11} + 2s_{12})T. \tag{9}$$

Consequently under stress there are only two transitions between this state and the ground state,

$$E_+ = h\nu_i + \Delta^{(i)}_{000} - \Delta^{(0)}_{000} + \tfrac{1}{2}\Delta^{(0)}_{111}, \tag{10}$$

$$E_- = h\nu_i + \Delta^{(i)}_{000} - \Delta^{(0)}_{000} - \tfrac{1}{2}\Delta^{(0)}_{111}, \tag{11}$$

denoted in order of energy as $i.1$ and $i.2$, from which

$$d_0 = \frac{\sqrt{3}}{s_{44}T}(E_+ - E_-), \tag{12}$$

$$a_i - a_0 = \frac{E_+ + E_- - 2h\nu_i}{2(s_{11} + 2s_{12})T}. \tag{13}$$

(3*b*) *Applied Force in a* ⟨100⟩ *Direction*

This analysis is identical to that for a ⟨111⟩ direction, with the shear deformation potential constant b replacing d in every instance and $s_{11} - s_{12}$ replacing $s_{44}/2\sqrt{3}$. Note that b_i, b_0 and $a_0 - a_i$ can be determined from a Γ_8 excited state, while only b_0 and $a_0 - a_i$ can be found from a Γ_6 or Γ_7 excited state, under ⟨100⟩ stress.

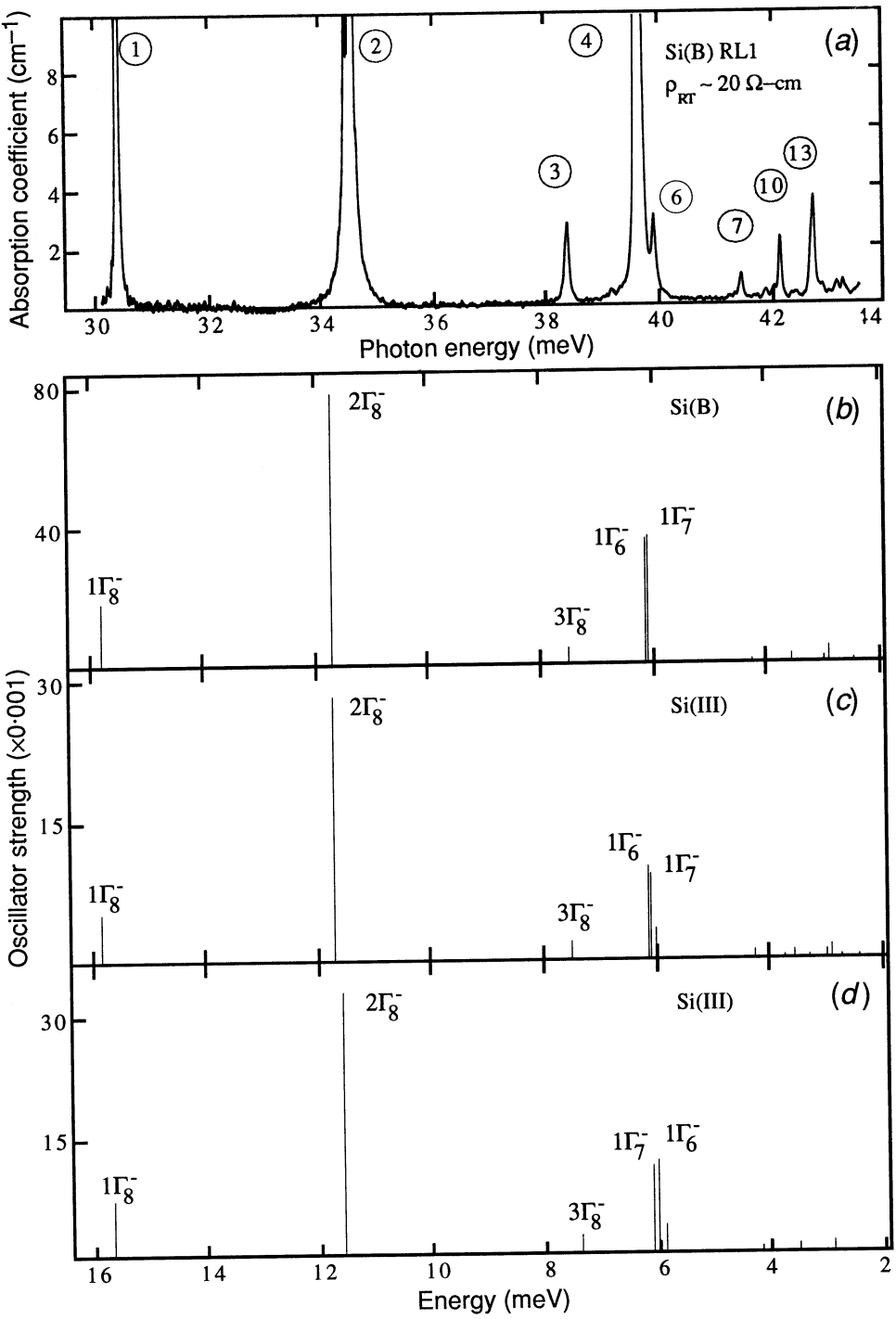

Fig. 2. (*a*) Unperturbed spectrum of Si(B). The coolant used was liquid helium. (*b*) Theory of Binggeli and Baldereschi (1989) for Si(B). (*c*) Theory of Binggeli and Baldereschi (1989) for Si(III). (*d*) Theory of Buczko and Bassani (1989) for Si(III).

Table 1. Energies, intensities and widths of spectral lines of boron in silicon

Labels				Transition Energies (meV)		Binding Energies (meV)					Oscillator Strengths ($x10^{-4}$)					Line Widths (μeV)
This work	Previous work[a,b]		Symmetry[c] (O_h)	This work[d]	Previous work[b,e]	This work[f]	Theory Si(B)[c]	Si(B)[g]	Si(III)[c]	Si(III)[h]	This work[i]	Theory Si(B)[c]	Si(B)[g]	Si(III)[c]	Si(III)[h]	This work
1	1	1	$1\Gamma_8^-$	30.371±0.004	30.37	15.78	15.78	15.79	15.78	15.63	-	180	177	51	73	-
2	2	2	$2\Gamma_8^-$	34.510±0.005	34.49	11.48	11.68	11.48	11.69	11.54	-	774	640	283	329	-
3	3	3	$3\Gamma_8^-$	38.379±0.006	38.35	7.47	7.48	7.24	7.48	7.35	-	51	54	21	28	-
4	4	4	$1\Gamma_6^-$	39.67±0.02	39.59	6.13	6.13	6.18	6.13	5.98	-	363	376	100	118	-
5	(4B)	4A	$1\Gamma_7^-$	-	39.67	-	6.09	6.23	6.09	6.08	-	366	260	92	112	-
6	4A	4B	$4\Gamma_8^-$	39.93±0.02	39.91	5.86	6.00	5.95	6.00	5.87	-	30	23	33	37	-
7	5	5	$5\Gamma_8^-$	41.474±0.001	41.47	4.25	4.25	4.24	4.25	4.17	13.0±0.1	13	17	8	11	58±1
8	-	6A	$2\Gamma_6^-$	41.913±0.001	41.91	3.80	3.82	3.81	3.82	3.70	3.7±0.1	0	12	2	-	63±2
9	-	6B	$6\Gamma_8^-$	42.060±0.001	42.06	3.64	3.69	3.84	3.69	3.63	3.2±0.1	3	0	5	5	33±2
10	6	6	$2\Gamma_7^-$	42.168±0.001	42.16	3.53	3.53	3.62	3.53	3.50	34.9±0.1	25	31	10	12	43.3±0.2
11	-	7	$7\Gamma_8^-$	42.423±0.001	42.41	3.27	3.27	3.33	3.27	3.24	2.9±0.1	2	3	3	5	59±3
12	-	-	$3\Gamma_6^-$	42.716±0.001	-	2.96	2.95	2.97	2.95	2.88	18.2±0.1	21	36	8	12	49±1
13	7	8	$3\Gamma_7^-$	42.761±0.001	42.74	2.92	2.87	3.07	2.87	2.86	46.3±0.1	51	6	14	17	48.7±0.2
14	-	8A	$8\Gamma_8^-$	42.922±0.001	42.92	2.75	2.71	2.85	2.71	2.67	4.0±0.1	5	0	4	5	65±2
-	-	-	$9\Gamma_8^-$	-	-	-	2.47	2.70	2.47	2.43	-	0	5	1	1	-
15	-	9A	$4\Gamma_6^-$	43.169±0.001	43.16	2.49	2.45	2.77	2.45	2.43	6.9±0.1	10	2	2	1	69±1
16	8	9	$4\Gamma_7^-$	43.282±0.001	43.24	2.37	2.37	2.88	2.37	2.35	9.1±0.1	9	42	4	5	52±1
17	-	-	-	43.378±0.002	-	2.27	-	-	-	-	0.9±0.1	-	-	-	-	31±8
18	-	-	$10\Gamma_8^-$	43.454±0.007	-	2.20	2.31	2.61	2.31	2.29	1.2±0.2	1	2	0	0	66±28
19	-	10A	$11\Gamma_8^-$	43.522±0.002	43.49	2.13	2.15	2.44	2.15	2.12	2.3±0.3	1	4	2	3	71±11
20	-	10B	$5\Gamma_6^-$	43.616±0.001	43.64	2.03	2.02	2.41	2.02	1.96	3.7±0.1	1	2	1	3	86±5
-	-	-	$12\Gamma_8^-$	-	-	-	1.92	2.36	1.92	1.91	-	0	0	0	0	-
-	-	-	$13\Gamma_8^-$	-	-	-	1.88	2.17	1.88	1.85	-	3	1	3	3	-
21	9	10	$5\Gamma_7^-$	43.729±0.001	43.71	1.91	1.88	2.50	1.88	1.87	12.0±0.1	28	12	8	9	53±1

Table 1. *continued*

22	-	10C	-	43.793±0.001	43.78	1.84	-	-	-	-	6.5±0.1	-	-	-	-	62±3
23	-	-	$6\Gamma_6^-$	43.865±0.001	-	1.77	1.77	2.07	1.77	1.76	5.1±0.2	19	4	4	4	59±3
-	-	-	$14\Gamma_8^-$	-	-	-	1.76	1.95	1.76	1.73	-	0	2	1	0	-
-	-	-	$6\Gamma_7^-$	-	-	-	1.73	2.04	1.73	1.71	-	2	9	1	1	-
-	-	-	$7\Gamma_6^-$	-	-	-	1.64	1.93	1.64	1.63	-	1	2	0	0	-
-	-	-	$15\Gamma_8^-$	-	-	-	1.62	1.88	1.62	1.60	-	1	1	0	0	-
24	-	10D	$7\Gamma_7^-$	43.965±0.004	43.95	1.67	1.62	1.92	1.62	1.61	2.4±0.1	5	5	2	2	-
-	-	11B	$16\Gamma_8^-$	-	44.20	-	1.54	1.61	1.54	1.52	-	0	2	0	0	-
-	-	-	$17\Gamma_8^-$	-	-	-	1.51	1.53	1.51	1.50	-	1	0	1	2	-
-	-	-	$8\Gamma_6^-$	-	-	-	1.46	-	1.46	1.42	-	0	-	0	0	-
-	-	-	$18\Gamma_8^-$	-	-	-	1.43	1.44	1.43	1.41	-	0	0	0	0	-
-	-	-	$9\Gamma_6^-$	-	-	-	1.42	-	1.42	1.39	-	0	-	1	1	-
-	-	-	$8\Gamma_7^-$	-	-	-	1.41	1.68	1.41	1.39	-	0	11	0	0	-
-	-	-	$19\Gamma_8^-$	-	-	-	1.37	1.35	1.37	1.36	-	0	0	0	1	-
-	-	-	$20\Gamma_8^-$	-	-	-	1.34	-	1.34	1.34	-	2	-	1	1	-
-	-	11	$9\Gamma_7^-$	-	44.27	-	1.30	1.55	1.30	-	-	16	1	5	-	-
-	-	-	$10\Gamma_6^-$	-	-	-	1.20	-	1.20	-	-	7	-	2	-	-
-	-	-	$10\Gamma_7^-$	-	-	-	1.19	-	1.19	-	-	0	-	0	-	-
25	10	-	-	44.408±0.002	-	-	-	-	-	-	7.1±0.0	-	-	-	-	737±16

[a] Onton *et al.* (1967). [b] Fischer and Rome (1983). [c]Binggeli and Baldereschi (1989). [d]Error estimates discussed in text. [e]Error is estimated to be ±0.02 meV for all lines except 10B and 11B where error is estimated to be ±0.05 meV. [f] Obtained by multiplying transition energy by -1.038 and adding 47.32 (see text for details). [g] Beinikhes *et al.* (1990). [h]Buczko and Bassani (1989) [i] Experimental line strengths (absorption coefficient x energy) have been normalised to an oscillator strength of 13 x 10^{-4} for line 7. To reconvert data to the units of cm^{-1} • meV, multiply data by 1026.

(3*c*) *Applied Force in Other Directions*

The splitting arising from uniaxial stress in an arbitrary direction is given by equation (15) of Chandrasekhar *et al.* (1973). Equation (28) of Chandrasekhar *et al.* gives the specific relationship

$$4(\Delta_{110}^{(i)})^2 = (\Delta_{100}^{(i)})^2 + 3(\Delta_{111}^{(i)})^2 . \tag{14}$$

Hence, if any two of $\Delta_{100}^{(i)}$, $\Delta_{110}^{(i)}$ or $\Delta_{111}^{(i)}$ are equal in magnitude then all three are, a situation termed by those authors as 'stress isotropy'.

4. Results and Discussion

(4*a*) *Unperturbed Spectrum*

The unperturbed spectrum of Si(B), the main features of which have been reported by many authors, is shown in Fig. 2*a*. It consists of a series of narrow absorption lines superimposed on a slowly increasing background.

The line labelling scheme employed here returns to the principle employed by Colbow (1963) of numbering the excitation lines from 1 in order of increasing transition energy. Colbow's original labels were adopted and extended by Onton *et al.* (1967) and others, but the labels have become increasingly cumbersome as additional features, unknown when the labels were first assigned, have been discovered. A case in point is line 4 of Colbow (1963), for which he observed a high energy shoulder; the shoulder was resolved by Onton *et al.* (1967) to be a distinct line, labelled by them 4A; Skolnick *et al.* (1974) discerned another line between these two, for which they appropriated the label 4A, relabelling the former 4A as 4B; Jagannath *et al.* (1981) returned the label 4A to the high energy line and used 4B for the intermediate one. It is not surprising that the most unwieldy set of labels accompanies the most detailed experimental results: for line 10, to maintain consistency with the old labels, Fischer and Rome (1983) have resorted to labels 10A to 10D, with line 10 itself falling between 10B and 10C, and to emphasise similarities between the spectra of different impurities in silicon these authors have relabelled the Si(B) line 7 as 8. In view of this increasing complexity and diversity of notation, and also in view of the exact agreement between experiment and present theory in the number of low energy lines, it is appropriate to return to the simple numbering principle of Colbow (1963) (see Table 1). In doing so, it is believed there will be no future change in the labels 1–7 (lines 4, 5, 6 correspond respectively to 4, 4B and 4A of Jagannath *et al.* 1981, and line 7 corresponds to line 5 of Colbow 1963), although label 8 and those beyond may require revision as further detail in the spectrum is resolved. [This relabelling was suggested by Lewis *et al.* (1988); the present lines 17, 18 and 25 were not included in that earlier work.] The small feature at ~39 meV is due to phosphorus impurities in the sample (see Jagannath *et al.* 1981) and is not accorded a number in the Si(B) series.

The experimental spectrum of Fig. 2*a* may conveniently be compared with the main features of some recent theoretical results presented in spectral form in Figs 2*b*, 2*c* and 2*d*, corresponding to the calculations of Binggeli and Baldereschi (1989) for Si(B), Binggeli and Baldereschi (1989) for Si(III), and Buczko and

Bassani (1989) for Si(III). The theoretical calculations based on the method of Baldereschi and Lipari (1973) use the notation stemming from $\bar{O}_h$ to label the states, rather than that of $\bar{T}_d$ utilised in the group-theoretical treatment. Reference to calculated states will adhere to the former notation. The label Si(III) means that these calculations were for group III impurities in general. The zero of hole energy has been set, for the purpose of this figure, to a transition energy of 45·86 meV. The ordinate ranges displayed have been chosen so that the strongest line ($2\Gamma_8^-$) is approximately equal in height in Figs 2*b*, 2*c* and 2*d*. It can be seen that the main features, in terms of line positions and strengths, agree well.

In examining the unperturbed spectrum of Si(B) our chief purpose has been to gather information about the weak and little-studied lines that crowd the high energy end of the spectrum. To facilitate this, samples offering high absorption, not well suited to measuring the intense low energy lines, have been prepared. Nonetheless, the transition energies of lines 1 to 3 have been remeasured and are given in Table 1. The original data points are equally spaced in wavelength and so the errors involved in determining the line energies are energy-dependent. The digitisation error is negligible (<0·0005 meV). The calibration of the spectrometer against the known wavelengths of water vapour (Cole 1977; see also Guelachvili and Rao 1986) is the chief uncertainty, the standard error from this source being estimated at 0·003 to 0·005 meV for lines 1 to 3. The reciprocal linear dispersion of the spectrometer multiplied by the slit width employed, ~0·017 meV, the diffraction limit of 0·007 to 0·010 meV, and the grating resolving power of 0·010 to 0·013 meV, are closely matched. The energy of an isolated line can be determined to at least one-tenth of these limits, and so they make only a small contribution to the overall uncertainty. It is seen in Table 1 that the energies of lines 1 to 3, for which the error is estimated to be 3 to 4 times less than that of Fischer and Rome (1983), agree within error with the latter's values. While an energy is listed for line 4 it is to be understood that this will represent a composite of lines 4 and 5, which have not, due to the deliberately high absorption of the samples used, been resolved in the present measurements. In summary, measurements of the positions of lines 1, 2, 3 and 6 have been made and agree with the most recent published data.

Fig. 3*a* shows the experimental spectrum for lines 7 and beyond, while Fig. 3*b* presents the theory of Binggeli and Baldereschi (1989) for Si(B) for comparison. The experimental data were obtained by adding 17 separate runs in order to increase the signal-to-noise ratio. In detail Fig. 3*a* is comparable, or slightly superior, to the spectrum shown as Fig. 4 of Fischer and Rome (1983).

To extract line positions in a region where many lines overlap, a curve-fitting program was used to analyse the spectrum. The curve-fitting program also gave line intensities and widths. It was assumed that each line can be described by a Lorentzian profile (see Jagannath 1980) and 20 of these profiles were adjusted to minimise the difference, in the least squares sense, between the experimental data and the computed fit to these. A constant underlying absorption background value of 0·17 cm^{-1} was also included in the computation. Fig. 3*a* shows the 20 Lorentzian profiles, and the sum of these and the constant offset (dashed curve), which follows closely the experimental data. The energies, intensities and widths

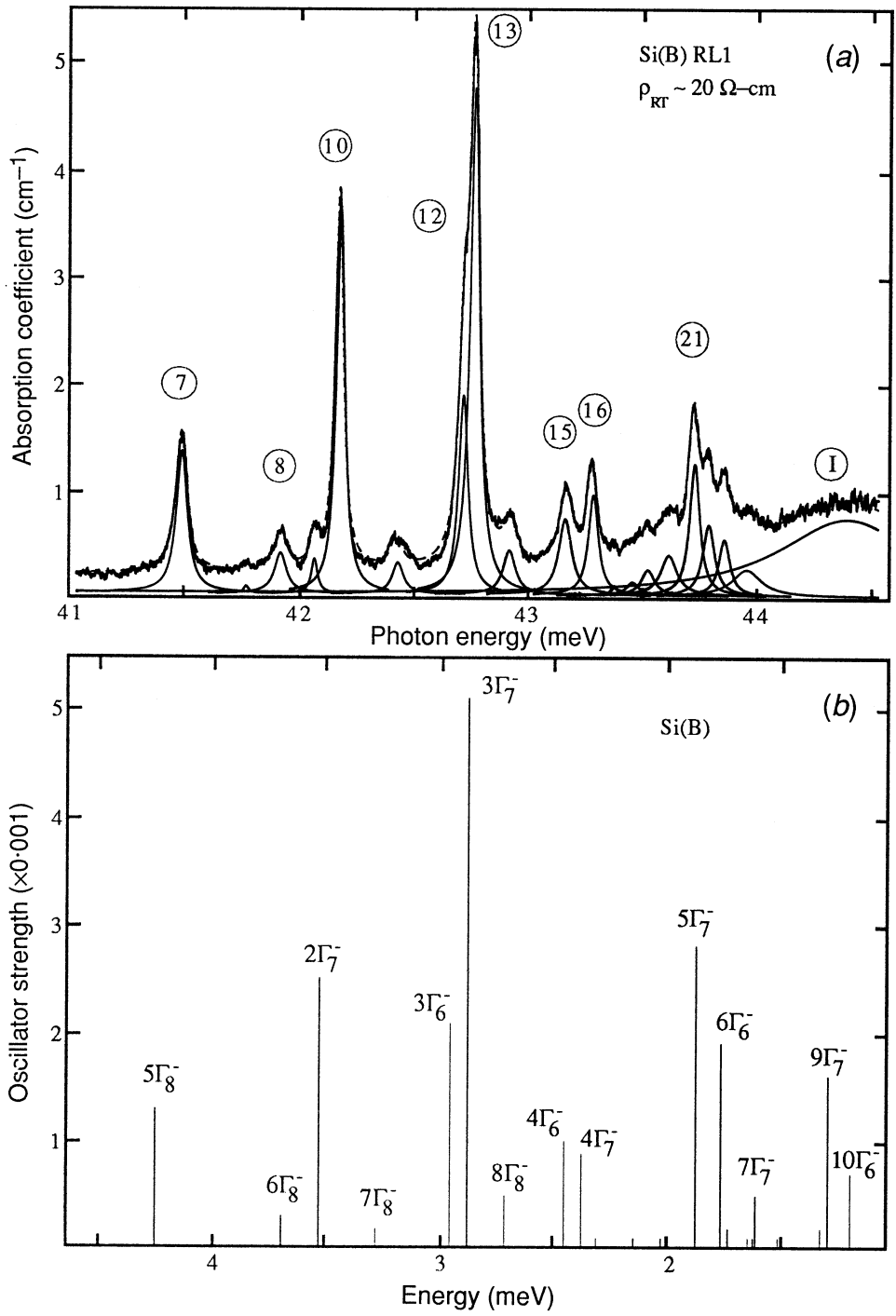

Fig. 3. (*a*) Detail of high energy transitions in the unperturbed spectrum of Si(B). (*b*) Theory of Binggeli and Baldereschi (1989) for Si(B).

obtained from this curve-fitting procedure are listed in Table 1. The errors given are the estimated standard errors arising in the fitting procedure. In the case of the energies, no other error source adds significantly to the standard error, the calibration error over this small wavelength range being $<0{\cdot}001$ meV; that the uncertainties in transition energy for lines 7 and above are generally less than those for lines 1 to 3 reflects the smaller uncertainty in the calibration and the curve-fitting, giving less error in ascertaining the peak position than the estimate used before for this of one-tenth of the spectral slit width.

In comparing the present line energies with those of Fischer and Rome (1983), the following remarks might be made. Lines 7, 8, 9, 10, 11, 13, 14, 15, 20, 21, 22 and 24 match, within experimental error, the Fischer and Rome lines 5, 6A, 6B, 6, 7, 8, 8A, 9A, 10B, 10, 10C and 10D, respectively. Although slightly outside the range of error estimates, it is probable that lines 16 and 19 correspond to their 9 and 10A respectively. We report several lines not recorded by Fischer and Rome: line 12, the low energy shoulder to the original line 7; lines 17, 18 and 23, small high energy lines; and line 25, which is included to account for the ionisation background. On the other hand, Fischer and Rome reported two lines which do not correspond to any in the present spectrum: the prominent line 11 and its small companion 11B. In short, these two most detailed sets of experimental line positions are in substantial agreement.

In order to compare the experimental results with theoretical calculations it is necessary to reconcile the experimental transition energies with the theoretical binding energies. In principle, these should sum to give the ionisation energy of the ground state, as the transition energies are measured in hole energy above the ground state, and the binding energies are measured in hole energy below the series continuum. In the event that the ionisation energy is not certain, which is the case, the transition and binding energies are usually pinned at a single energy—usually that of a strong isolated line (see e.g. Ramdas and Rodriguez 1981). However, it has been noted previously (Lewis *et al.* 1988), and is evident in Figs 2 and 3, that the energy *scaling* may differ between the experimental and theoretical energies—in the language of geometry, not only is the intercept non-zero, but also the gradient is non-unity, of the locus of energies plotted on the theory–experiment plane. Hence a method of fitting a curve to the data pairs consisting of the experimental transition energy, $h\nu$, and the theoretical binding energy, ϵ_b, for each of the lines 1, 2, 3, 7 and 10 is adopted. Using the data of Binggeli and Baldereschi (1989) to represent the theory, it is found that the point given by line 2 is slightly removed from the straight line given by the other four, and so is discarded for the correlation. The remaining four points lie on a straight line (correlation coefficient $0{\cdot}999998$) and yield

$$\epsilon_b(\text{exp}) = 47{\cdot}32 \pm 0{\cdot}05 - (1{\cdot}038 \pm 0{\cdot}001)h\nu\,. \tag{15}$$

This equation is used in Table 1 to convert the experimental transition energies to experimental binding energies. A similar calculation was carried out using the theoretical data of Beinikhes *et al.* (1990), yielding an intercept of $47{\cdot}21{\pm}0{\cdot}19$, gradient $-(1{\cdot}035{\pm}0{\cdot}005)$ and correlation coefficient $0{\cdot}99997$. In fitting to these data, line 3 does not quite fall on the straight line given by the other points and so only lines 1, 2, 7 and 10 were used.

In general terms, many more theoretical states have been calculated than observed, but many states in common can be identified with most of the experimental data lying within 0·02 meV of the corresponding theoretical data.

In comparing in detail the experimental and calculated line energies and strengths the following is observed. Lines 1, 2, 3, 6, 7, 10, 11 and 12 can be identified with transitions to the $1\Gamma_8^-$, $2\Gamma_8^-$, $3\Gamma_8^-$, $4\Gamma_8^-$, $5\Gamma_8^-$, $2\Gamma_7^-$, $7\Gamma_8^-$ and $3\Gamma_6^-$ states, respectively, in each of the theoretical analyses. Line 4 corresponds to $1\Gamma_7^-$ and line 5 to $1\Gamma_6^-$, according to Buczko and Bassani (1989) and Beinikhes *et al.* (1990), the reverse of the ordering given by Binggeli and Baldereschi (1989). Similarly the results of Buczko and Bassani (1989) and Binggeli and Baldereschi (1989) suggest line 8 corresponds to $2\Gamma_6^-$ and line 9 to $6\Gamma_8^-$, while Beinikhes *et al.* (1990) have the reverse ordering. Piezospectroscopic measurements can, in principle, reveal the order of the states in dispute. However, in the present measurements, the line 4–5–6 complex has not been studied, and indeed is formidable, having up to eight stress-induced components, although in a similar case, the C-line of Ge(Ga), ten components, including even parity states, have been successfully identified (Vickers *et al.* 1988). Recently Piao (1992), on the basis of piezospectroscopic measurements on Si(In), has concluded that lines 4 and 4A in that system have symmetries of $1\Gamma_7^-$ and $1\Gamma_6^-$ respectively. The piezospectroscopic results for lines 8 and 9 are discussed later. Thus, of the first 12 lines, the ordering of two pairs is in doubt, and eight are clearly identified with theoretically calculated states.

Beyond line 12 the agreement between theories, and between theory and experiment, is not as complete. Considering both the energies and strengths of the various lines in comparing with the theory of Binggeli and Baldereschi (1989), one can identify lines 13 to 24, in sequence, with states $3\Gamma_7^-$, $8\Gamma_8^-$, $4\Gamma_6^-$, $4\Gamma_7^-$, none, $10\Gamma_8^-$, $11\Gamma_8^-$, $5\Gamma_6^-$, $5\Gamma_7^-$, none, $6\Gamma_6^-$ and $7\Gamma_7^-$. The theory of Buczko and Bassani (1989) gives the same outcome, except for the identification of line 22 with $13\Gamma_8^-$ and 24 with $15\Gamma_8^-$. It is possible that state $10\Gamma_8^-$ could be associated with line 17, to which it is closer in energy than to line 18; however, the identification has been made on the basis of the slightly greater strength of line 18, leaving no theoretical state for line 17. In the theory of Binggeli and Baldereschi (1989) no state corresponds to line 22, unless line 21 is $13\Gamma_8^-$ and 22 is $5\Gamma_7^-$, which is untenable on the basis of the oscillator strengths. Many calculated transitions are not seen in the experimental spectrum—18 are missing when the comparison is made with the calculations of Binggeli and Baldereschi (1989) and 15 for Buczko and Bassani (1989). All of these unobserved transitions have very small strengths, except for $10\Gamma_6^-$ and $9\Gamma_7^-$, which both lie close to line 11 of Fischer and Rome (1983).

Alternatively, beyond line 12, one can use the theory of Beinikhes *et al.* (1990) to identify successive experimental lines as $4\Gamma_7^-$, $8\Gamma_8^-$, $5\Gamma_7^-$, $11\Gamma_8^-$, $5\Gamma_6^-$, $12\Gamma_8^-$, $13\Gamma_8^-$, $6\Gamma_6^-$, $6\Gamma_7^-$, $14\Gamma_8^-$, $7\Gamma_6^-$ and $8\Gamma_7^-$. This assignment is quite different to that based on the other two theories. It does, however, assign a state to every line. The above assignment differs in some instances with how Table 1 of Beinikhes *et al.* (1990) identifies the lines of Fischer and Rome (1983), replacing the second '8' in that table with '8A' (the first '8' being the present line 13) and interchanging the first '9' with energy 2·60 meV in that table, the present line 15 ($5\Gamma_7^-$), and '9A', with energy given as 2·52 meV, the present line 16

($11\Gamma_8^-$). Hence lines 17, 18 and 23, not observed by Fischer and Rome (1983), are assigned. As with the other theories, there are many lines calculated but not observed; none of these has a very large oscillator strength.

Apart from the energies of the individual transitions, it is of interest to establish the series limit, which is the binding energy of the ground state. This may be done in several ways. First, as already mentioned, a theoretical binding energy can be added to the experimental transition energy of a chosen line. Recently, for example, Yu *et al.* (1989) added their value (42·16±0·01 meV) for our line 10 to the binding energy given by Lipari *et al.* (1980) to deduce the ground state binding energy to be 45·83±0·01 meV. A problem with this approach, as intimated above, is that different lines give different results. This has suggested a second method since the difference is systematic and can be expressed in a form like equation (15). Solving this for zero binding energy yields 45·57±0·01 meV and solving for zero transition energy, 47·32±0·05 meV; fitting instead to the theory of Beinikhes *et al.* (1990) gives these energies as 45·62±0·05 and 47·21±0·19 meV respectively. The values given by this hybrid of experiment and theory might be compared with the estimate of Beinikhes *et al.* (1990) of 45·79 meV. Thirdly, Fischer and Rome (1983) have proposed that a spectroscopic feature indicates the ionisation edge, which they give as 44·39 meV. However our spectra, and others published, do not show this feature. Moreover, Yu *et al.* (1989) claim to have observed discrete lines at energies higher than this, and thus infer that the ionisation energy is >44·39 meV.

In relation to the ionisation energy, a remark might be made about modelling the rising background on which the distinct absorption lines are superimposed. This background is evident in all of the reported spectra of Si(B). That the background is not due to the lattice or otherwise intrinsic to Si is evident from a variety of experiments: it appears only at low temperatures (Colbow 1963); it does not occur in samples containing principally other impurities [e.g. Si(As), Jagannath *et al.* 1981, and Si(Li), Jagannath and Ramdas 1980], although such samples exhibit their own absorption increase at the high energy end of their series. Hence, the background is attributable to the doping. To model this background, made of an infinite number of therefore closely spaced transitions of low intensity, a single additional Lorentzian peak was chosen, line 25 in Table 1. A Gaussian profile might have been the preferred shape, but the difference this would make to curve fitting would not be large (Posener 1959); alternatively, a polynomial expression might have been used, presumably with comparable error. While not suggesting that this final peak corresponds to the series limit, it is of interest to compare its energy, 44·41 meV, with the value for the ionisation energy suggested by Fischer and Rome (1983), namely 44·39 meV.

The full widths at half height for lines 7 to 23 are given in the final column of Table 1. These fall in the range 30–90 μeV, with most in the range 40–70 μeV. No comprehensive measurement or theoretical predictions of these line widths are known.

(4*b*) *Piezospectroscopy*

Figs 4 to 14 and Table 2 give the experimental results for the piezospectroscopy of lines 1, 2, 3, 7 and 10. The normal pattern is to first present spectra showing the splitting pattern, then a fan diagram showing the behaviour of the

Table 2. Deformation potential constants (eV) of states of boron in silicon

Line (i)	Authors	<111> direction		<100> direction		isotropic
		d_o	d_i	b_o	b_i	$a_i - a_o$
1	Present	-4.02±0.08	-1.76±0.05	-1.34±0.02	-0.055±0.010	-0.41±0.07
	(Chandrasekhar *et al.* 1973)		-2.31±0.25		0.20±0.15	
	(Buczko 1987)		-1.84		-0.025	
2	Present	-3.93±0.10	1.36±0.07	-1.98±0.08[a]	1.53±0.12[a]	0.86±0.10
	(Chandrasekhar *et al.* 1973)	-4.46±0.10	2.64±0.25		1.61[b]	
	(Buczko 1987)		2.04		1.09	
3	Present	-4.10±0.10	-2.1±0.3[c]	-1.42±0.03	0.03±0.10[c]	-2.17±0.13[c]
	(Buczko 1987)		-1.70		0	
7	Present	-3.82±0.11	-2.1±0.2[c]	-1.27±0.04	0.01±0.14[c]	-1.0±0.7[c]
	(Buczko 1987)		-1.65		0	
10	Present	-3.70±0.09	none	-1.28±0.04	none	1.1±0.7[c]
all	Present (lines 1, 2, 3, 7, 10)	-3.91±0.07		-1.46±0.13		
	(Chandrasekhar *et al.* 1973)	-4.50±0.15[d]		-1.61±0.07[d]		
	(Buczko 1987)	-4.17		-1.39		

[a]Magnitude deduced from <111> and <110> data; sign as given by Buczko (1987). [b]Estimated as being equal in magnitude to the ground state splitting. [c]Second order polynomial fit. [d]Deduced from 2p' data.

energies of the various components as a function of stress, then the differences of the energies of components that permit the determination of the shear deformation potential constants, and finally an addition of components that permits the determination of the relative difference between the hydrostatic deformation potential constants of the ground and excited states.

The data for stress in the ⟨111⟩ direction are given first. As may be seen from Fig. 1 the polarisation pattern in this direction is, in general, slightly simpler and without the ambiguity that is present for the ⟨100⟩ direction, admitting a maximum of five rather than six transitions between any two states. The results for the ⟨100⟩ direction are given next. Using stress in this direction it is possible to distinguish Γ_6 and Γ_7 states, which give identical polarisation features under ⟨111⟩ stress (see Fig. 1). For line 2 only, which exhibits little splitting for $\boldsymbol{F} \parallel \langle 100 \rangle$, results are presented for $\boldsymbol{F} \parallel \langle 110 \rangle$.

It has been shown (see Onton *et al.* 1967) that the ground state is of Γ_8 symmetry and that under ⟨111⟩ compression the Γ_4 substate is of lower energy than the Γ_{5+6}. Under ⟨100⟩ compression, the ordering of the substates of the

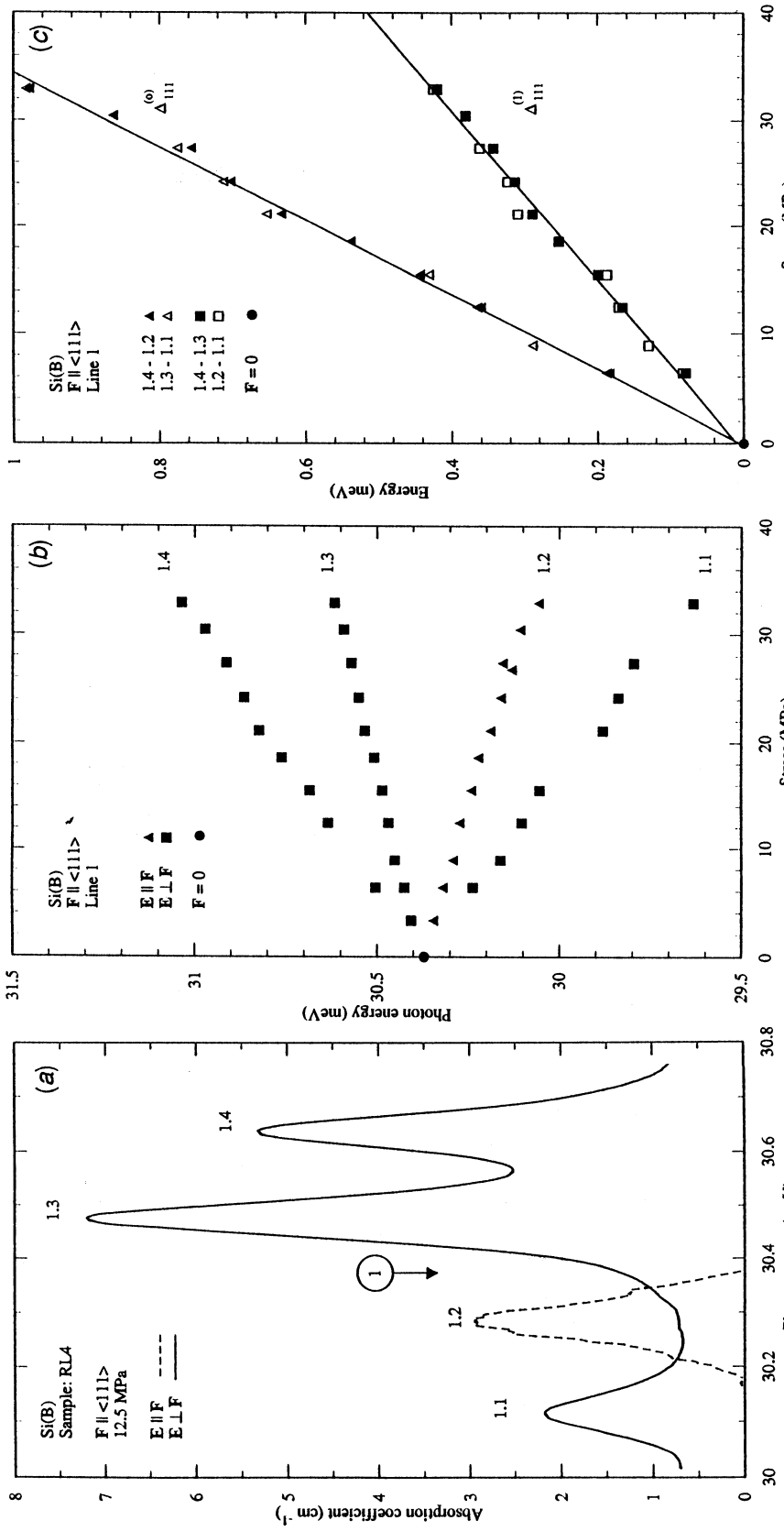

Fig. 4. (*a*) Effect of ⟨111⟩ compression on the spectrum of line 1. (*b*) Stress dependence of the energies of the components of line 1 under ⟨111⟩ compression. (*c*) Stress splitting of the ground and excited states as deduced from the components of line 1 under ⟨111⟩ compression.

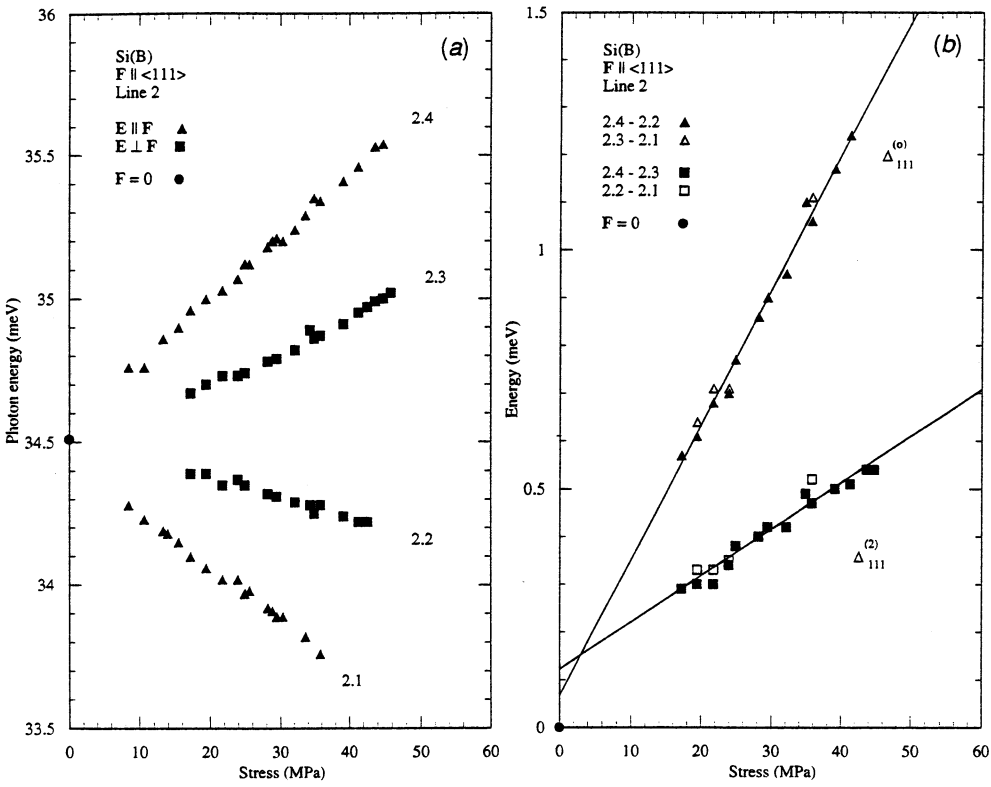

Fig. 5. (*a*) Stress dependence of the energies of the components of line 2 under ⟨111⟩ compression. (*b*) Stress splitting of the ground and excited states as deduced from the components of line 2 under ⟨111⟩ compression.

ground state is taken to be that predicted from the known behaviour of the valence band edge; thus the Γ_7 substate is of lower energy than the Γ_6 (see e.g. Buczko 1987). The symmetry of each state, and the relative magnitudes of the ground and excited state splittings, will be deduced using the information summarised in Fig. 1. The ordering of the substates of a given unperturbed state determines the sign of the deformation potential constants.

(i) Force applied in a ⟨111⟩ direction. For $\boldsymbol{F} \parallel \langle 111 \rangle$, the spectrum for line 1 (Fig. 4*a*) is similar to that shown in Fig. 17 of Onton *et al.* (1967) with all three allowed components for $E_\perp$ and a fourth component for $E_\parallel$. Chandrasekhar *et al.* (1973) reported a similar spectrum (their Fig. 6) but without data for component 1.1. From the selection rules (Fig. 1) it is clear that the orderings of the ground and excited states are the same and the component 1.2, missing for $E_\perp$, must be a $\Gamma_{5+6} \rightarrow \Gamma_{5+6}$ transition. The absence of component 1.3 for $E_\parallel$ suggests that the intensity parameter $u_1 \sim 1$. (The subscript corresponds to the line number.) From the stress dependence of the intensities of the components, it is deduced (see Onton *et al.* 1967; Chandrasekhar *et al.* 1973) that both the components 1.1 and 1.2 originate from the upper substate of the ground state and thus the upper substate is the Γ_{5+6} state.

In Fig. 4*c*, straight lines have been fitted to the appropriate differences in components that yield the stress splitting of the ground and excited states. The

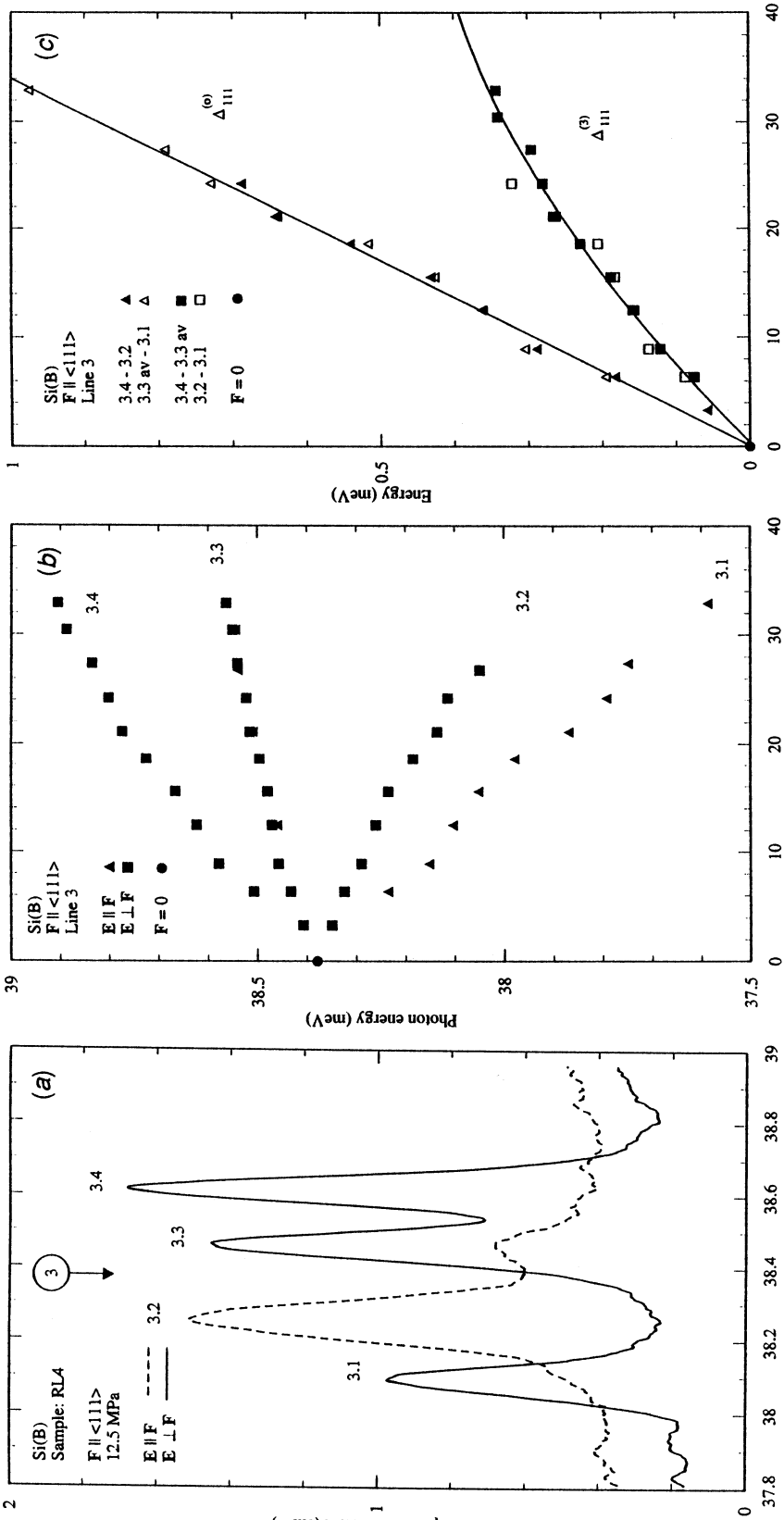

Fig. 6. (*a*) Effect of ⟨111⟩ compression on the spectrum of line 3. (*b*) Stress dependence of the energies of the components of line 3 under ⟨111⟩ compression. (*c*) Stress splitting of the ground and excited states as deduced from the components of line 3 under ⟨111⟩ compression.

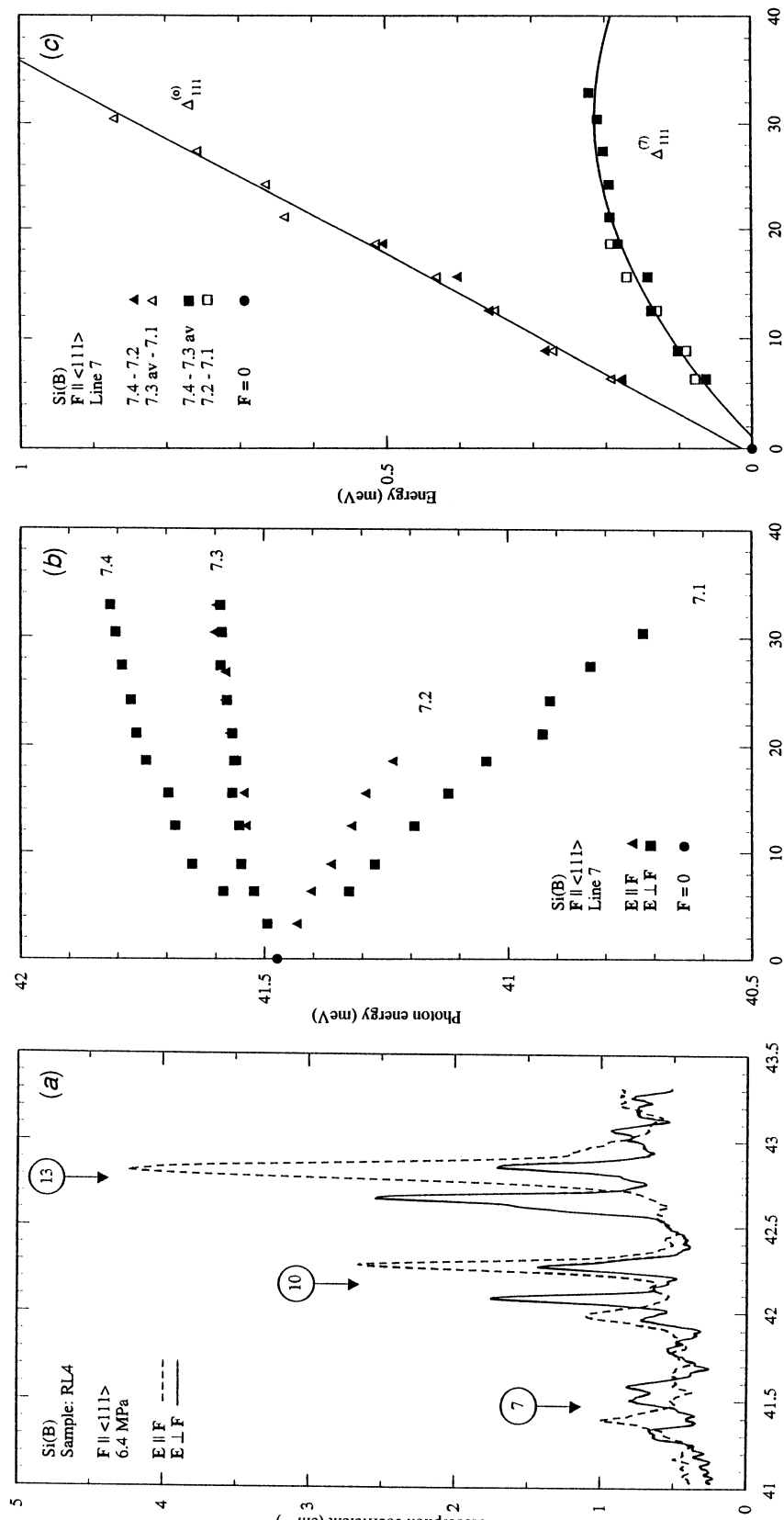

Fig. 7. (*a*) Effect of ⟨111⟩ compression on the spectrum of lines 7 and beyond. (*b*) Stress dependence of the energies of the components of line 7 under ⟨111⟩ compression. (*c*) Stress splitting of the ground and excited states as deduced from the components of line 7 under ⟨111⟩ compression.

symbols indicate which pairs of components have been used in obtaining each datum point, but the complete set is employed to find the line of best fit. (The zero stress point is shown for reference, but it is not used in the curve-fitting.) The values thus deduced for d_0 and d_1 are given in Table 2, which also contains the values obtained experimentally by Chandrasekhar *et al.* (1973) and theoretically by Buczko (1987). It is seen that the previous experimental value of d_1 is approximately 30% higher than the present value, while the theoretical value is about 5% higher. Both these differences are beyond the standard error estimate arising from the fitting of the present data with straight lines.

The spectra for line 2 under ⟨111⟩ stress reveal that component 2.1 occurs for $E_{\|}$ only, components 2.2 and 2.3 appear for $E_{\perp}$ only, while 2.4 is observed for both polarisations. This accords with the spectra of Onton *et al.* (1967), and hence with the ordering (opposite to that for the ground state) and magnitude (smaller than that for the ground state) of the excited state splitting deduced by them for line 2. The weak component, 2.4, for $E_{\perp}$ is predicted to have a relative intensity of $u_2/2$ (see Fig. 1) which suggests $u_2 \sim 0$ and accounts for the robustness of the other four components. As before for line 1, the slopes of straight lines fitted to the stress splitting data (Fig. 5*b*) are used to calculate the deformation potential constants which are given in Table 2. Again the present values are smaller in

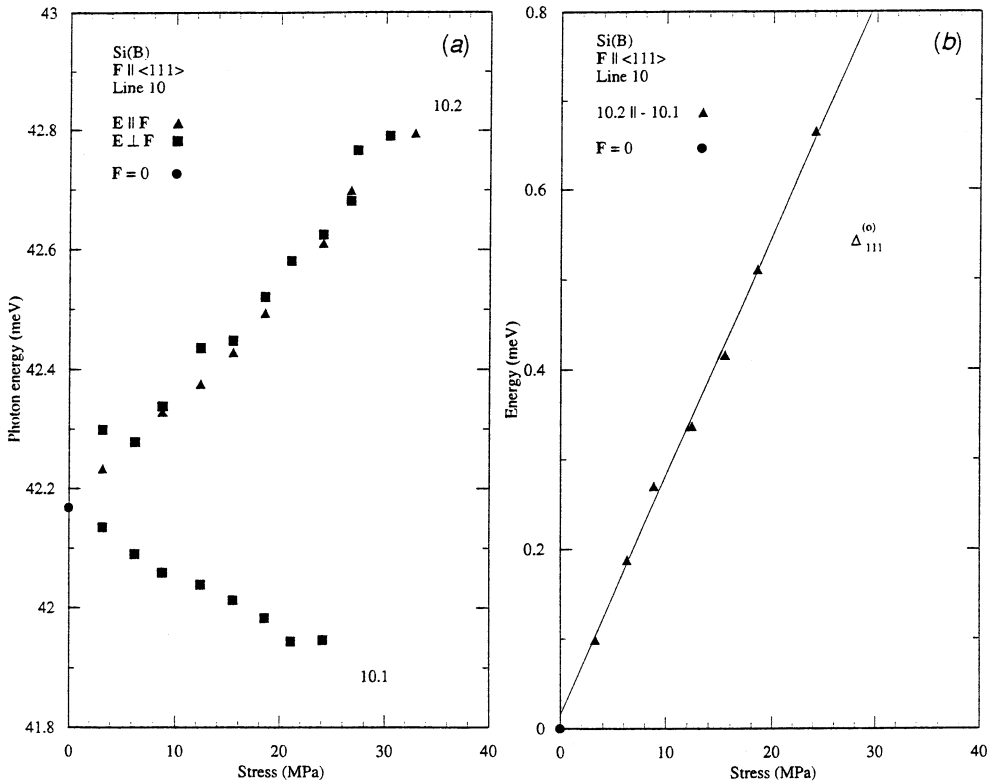

Fig. 8. (*a*) Stress dependence of the energies of the components of line 10 under ⟨111⟩ compression. (*b*) Stress splitting of the ground state as deduced from the components of line 10 under ⟨111⟩ compression.

magnitude than those given in the previous work, being about half the value obtained experimentally and about two-thirds of the calculated value.

The quantitative piezospectroscopy of line 3 has not been previously reported, although Onton *et al.* (1967) noted that the polarisation pattern is identical to that of line 1. This is in accord with the present observations, with the exception that component 3.3, while weak, is observed here for $E_{\|}$ (Fig. 6*a*). The assignment of symmetry and the remarks made above concerning the intensities of the components of line 1 apply to line 3 also. In fitting the data of the excited state splitting (Fig. 6*c*) a second-order, rather than first-order, polynomial was required. The resultant deformation potential constant (given in Table 2) is close to that calculated by Buczko (1987).

A spectrum for lines 7 and beyond is shown in Fig. 7*a*. The behaviour of line 7 follows the same pattern as that of lines 1 and 3, with the same ordering. As was the case for line 3, a parabolic fit is made to determine the excited state splitting (Fig. 7*c*), with an identical result to that for line 3. This compares well with the calculations of Buczko (1987) which also show that $d_7 \approx d_3$.

Line 10 shows only two components and is identified as either a Γ_6 of Γ_7 state, neither of which splits under stress. It cannot be a Γ_8 state, as comparison of the possible splitting patterns (Fig. 1) and the experimental data (Fig. 8) indicate.

Of the higher energy lines, 12 to 16 follow the same pattern as line 10. Line 8 probably corresponds to either a Γ_6 or Γ_7 state. There are no clear data for line 11 and those lines beyond 16. The greatest problem in interpreting the higher energy experimental piezospectroscopic data is that there are more components evident for $E_{\|}$ than there are for $E_{\perp}$, a pattern not consistent with any transition scheme shown in Fig. 1.

The analysis of Buczko (1987) gave a value of $d_0 = -4{\cdot}17$ eV for one of the ground state deformation potential constants, while Chandrasekhar *et al.* (1973) estimated this to be $-4{\cdot}50 \pm 0{\cdot}15$ eV from the stress splitting of the 2p′ line and $-4{\cdot}46 \pm 0{\cdot}10$ eV from the splitting of line 2. The ground state splitting has been computed from the present data using linear fits to data from each of lines 1, 2, 3, 7 and 10—detailed results are set out in Table 2—and combining the data for these leads to $d_0 = -3{\cdot}91 \pm 0{\cdot}07$ eV, close to Buczko's value and about 90% of the Chandrasekhar *et al.* value but not, within error, agreeing with either.

(ii) Force applied in a ⟨100⟩ direction. The spectra for line 1 for $\boldsymbol{F} \parallel \langle 100 \rangle$ are shown in Fig. 9*a*. Evidently the transitions for the two polarisations almost coincide, but closer inspection reveals that the components for $E_{\|}$ bracket those for $E_{\perp}$; this small but distinct separation is also evident in the spectra and fan charts of Onton *et al.* (1967) and Chandrasekhar *et al.* (1973). As the two components for $E_{\|}$ (1.1 and 1.4) are the extreme ones, the ordering of the excited state must be the same as that of the ground state, in agreement with Onton *et al.*, but in contrast to Chandrasekhar *et al.* who, in a numerical comparison with the splitting of the 2p′ line, concluded that the ground and excited states of line 1 are ordered oppositely. The ground and excited state splittings are shown in Fig. 9*c*. The very small splitting of the excited state is evident, resulting in a deformation potential constant close to zero, in agreement with the value of Buczko (1987) (see Table 2).

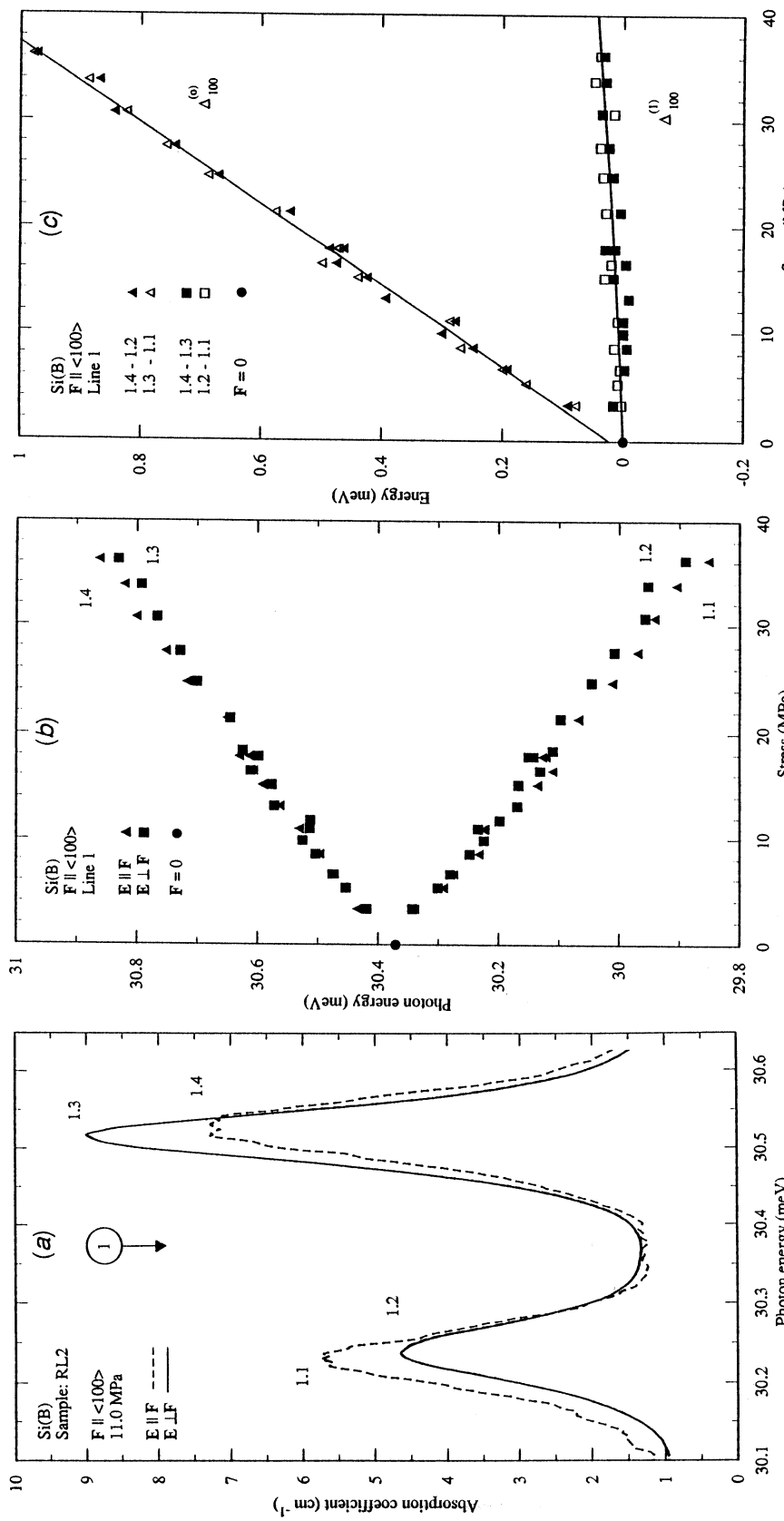

Fig. 9. (*a*) Effect of ⟨100⟩ compression on the spectrum of line 1. (*b*) Stress dependence of the energies of the components of line 1 under ⟨100⟩ compression. (*c*) Stress splitting of the ground and excited states as deduced from the components of line 1 under ⟨100⟩ compression.

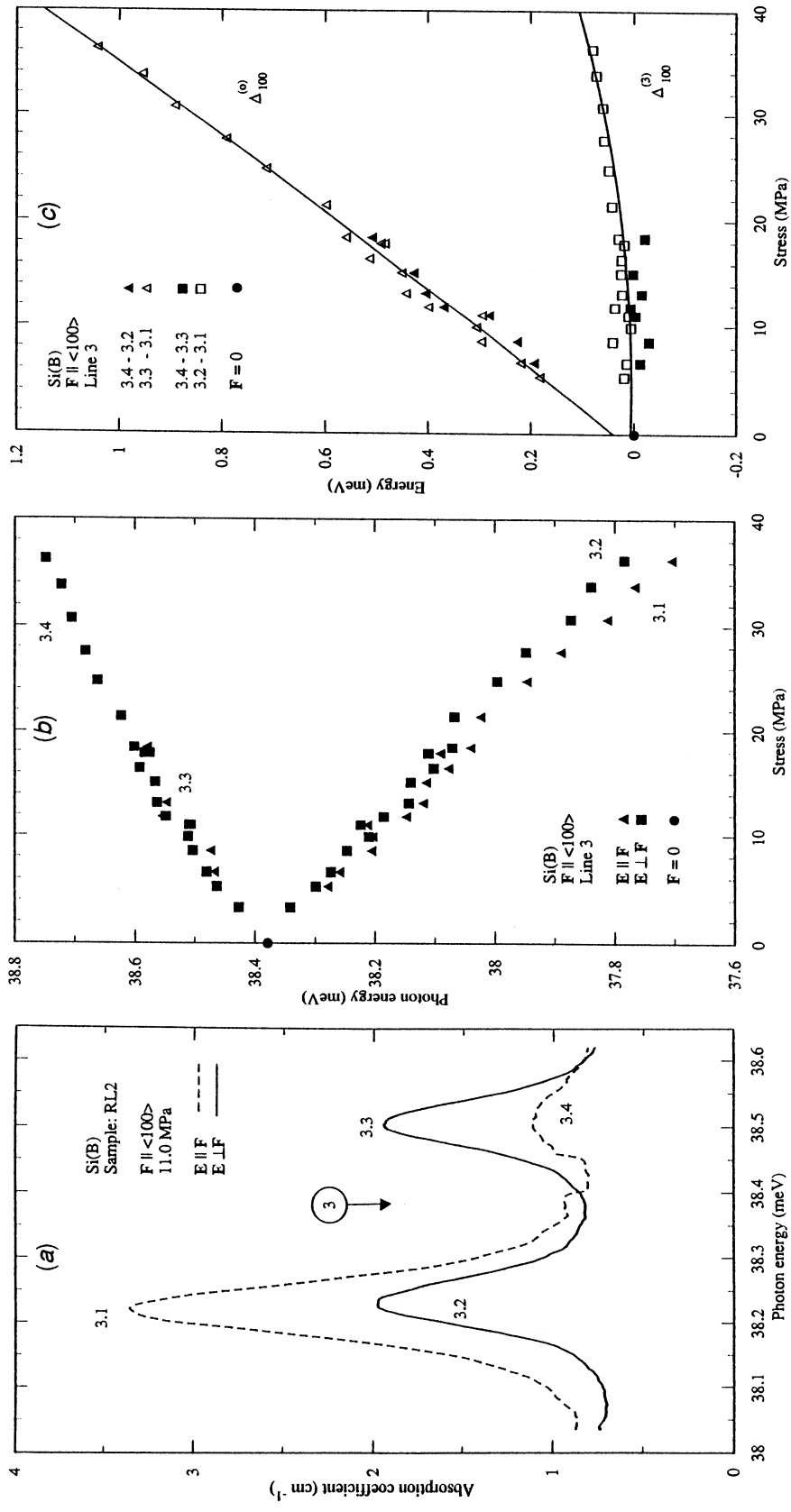

Fig. 10. (*a*) Effect of ⟨100⟩ compression on the spectrum of line 3. (*b*) Stress dependence of the energies of the components of line 3 under ⟨100⟩ compression. (*c*) Stress splitting of the ground and excited states as deduced from the components of line 3 under ⟨100⟩ compression.

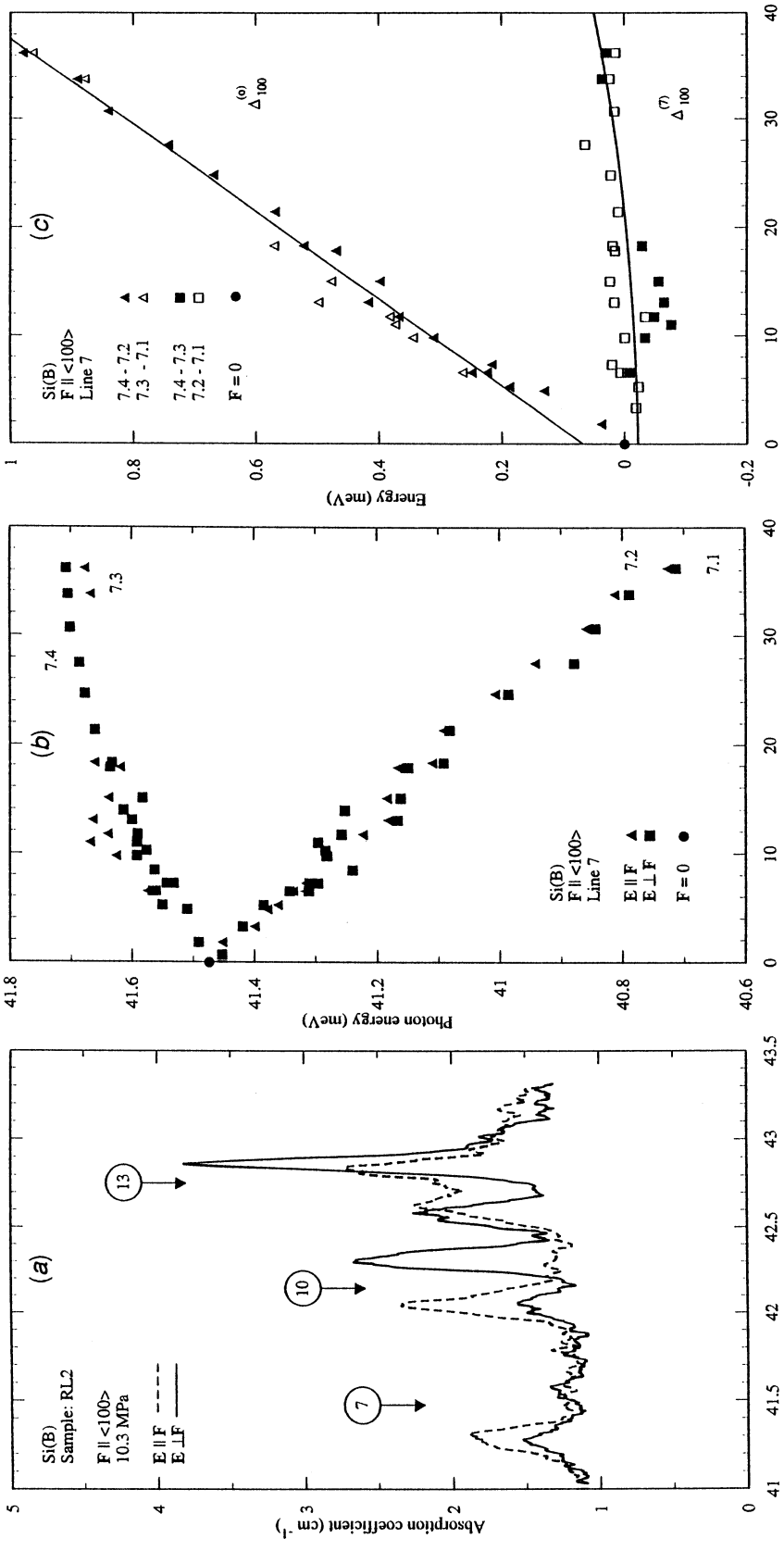

Fig. 11. (*a*) Effect of ⟨100⟩ compression on the spectrum of line 7 and beyond. (*b*) Stress dependence of the energies of the components of line 7 under ⟨100⟩ compression. (*c*) Stress splitting of the ground and excited states as deduced from the components of line 7 under ⟨100⟩ compression.

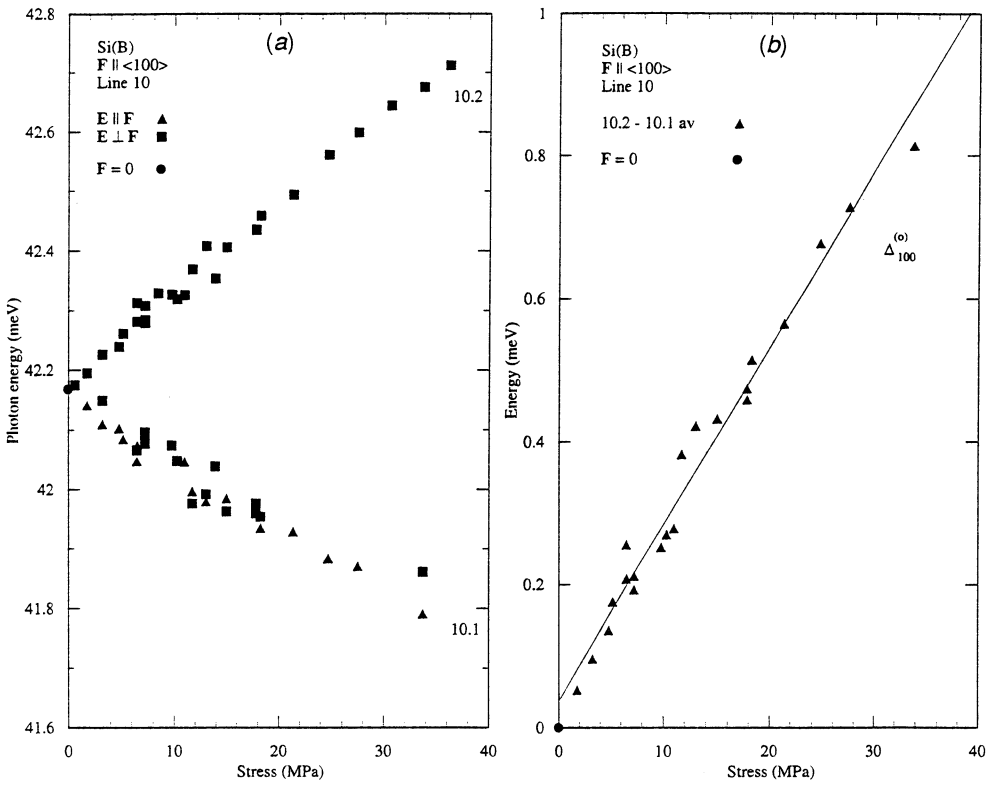

Fig. 12. (*a*) Stress dependence of the energies of the components of line 10 under ⟨100⟩ compression. (*b*) Stress splitting of the ground state as deduced from the components of line 10 under ⟨100⟩ compression.

The stress splitting of line 3 is measured here quantitatively for the first time (Fig. 10). Its symmetry and ordering are deduced to be the same as those of line 1. The intensities also follow the pattern of line 1, in that the two components for $E_\perp$ are approximately equal in intensity; however, for $E_\parallel$, component 3.1 is about 8 times the intensity of component 3.4. The polarisation features indicate a negative value for b_3, but the second-order fit to the data (Fig. 10*c*) gives a positive value. The value determined from this graph, $b_3 = (0{\cdot}03 \pm 0{\cdot}10)$ eV, embraces the value of zero computed by Buczko (1987).

For line 7, in contrast to lines 1 and 3, the components for $E_\perp$ bracket those for $E_\parallel$ (Fig. 11*a*), and hence the splitting of the excited state is in the opposite order to that of the excited states of lines 1 and 3. As for line 3, line 7 shows very little excited state splitting, and the value given in Table 2 for b_7 is consistent with the value of zero given by Buczko (1987).

Line 10 shows the 'classic' pattern of a split Γ_6 or Γ_7 state, with the more energetic component for $E_\perp$ being $\sim$3 times the intensity of the less energetic (Fig. 12*a*). These data establish that line 10 has Γ_7 symmetry, thus verifying the theoretical assignment for this state (see Table 1).

Of the higher lines, 11 to 14 appear to be Γ_8, Γ_6, Γ_7 and Γ_8 respectively, but this is not well established. Even less certain is the assignment of lines 8, 9

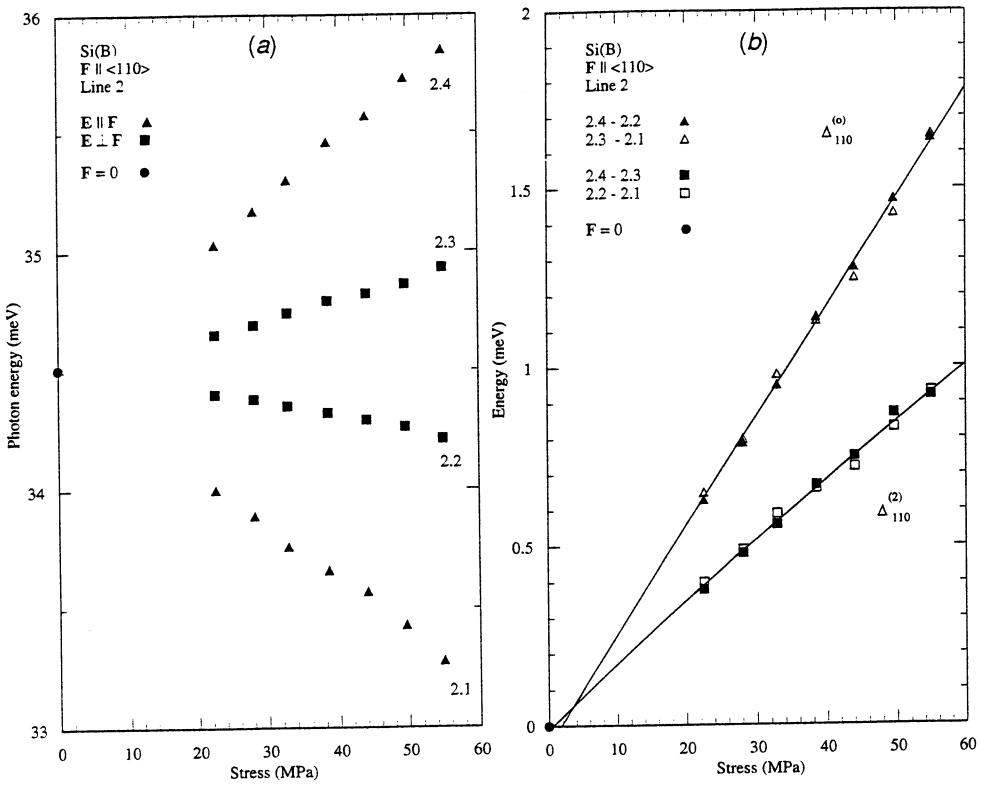

Fig. 13. (*a*) Stress dependence of the energies of the components of line 2 under ⟨110⟩ compression. (*b*) Stress splitting of the ground and excited states as deduced from the components of line 2 under ⟨110⟩ compression.

and 10. Once again, a dearth of components for $E_\perp$ inhibits the interpretation of the experimental data.

As for ⟨111⟩ stress, an experimental determination has been made of the ground state deformation potential constant using data from each of the lines 1, 2, 3, 7 and 10; the results are listed in Table 2. The final value of $b_0 = -1{\cdot}46 \pm 0{\cdot}13$ eV agrees, within error, with the calculation of Buczko (1987) and is about 90% of the value of Chandrasekhar *et al.* (1973), again in agreement, within the error.

(iii) Force applied in a ⟨110⟩ direction. For $\boldsymbol{F} \parallel \langle 110 \rangle$, line 2 follows the polarisation pattern shown in Fig. 20*a* of Onton *et al.* (1967). The stress splitting of the components is shown in Fig. 13*a*. The ground and excited state stress splittings are shown in Fig. 13*b*. The values of b_0 and b_2 determined by combining these data and the ⟨111⟩ data using equation (14) appear in Table 2.

(iv) Isotropic stress. As discussed in the theory section, by appropriate summation of the energies of the stress-induced components, for stress applied in either the ⟨100⟩ or ⟨111⟩ direction, the difference between the excited and ground state hydrostatic deformation potential constants, $a_i - a_0$, can be determined, but for no direction of applied stress can a_i or a_0 be determined independently.

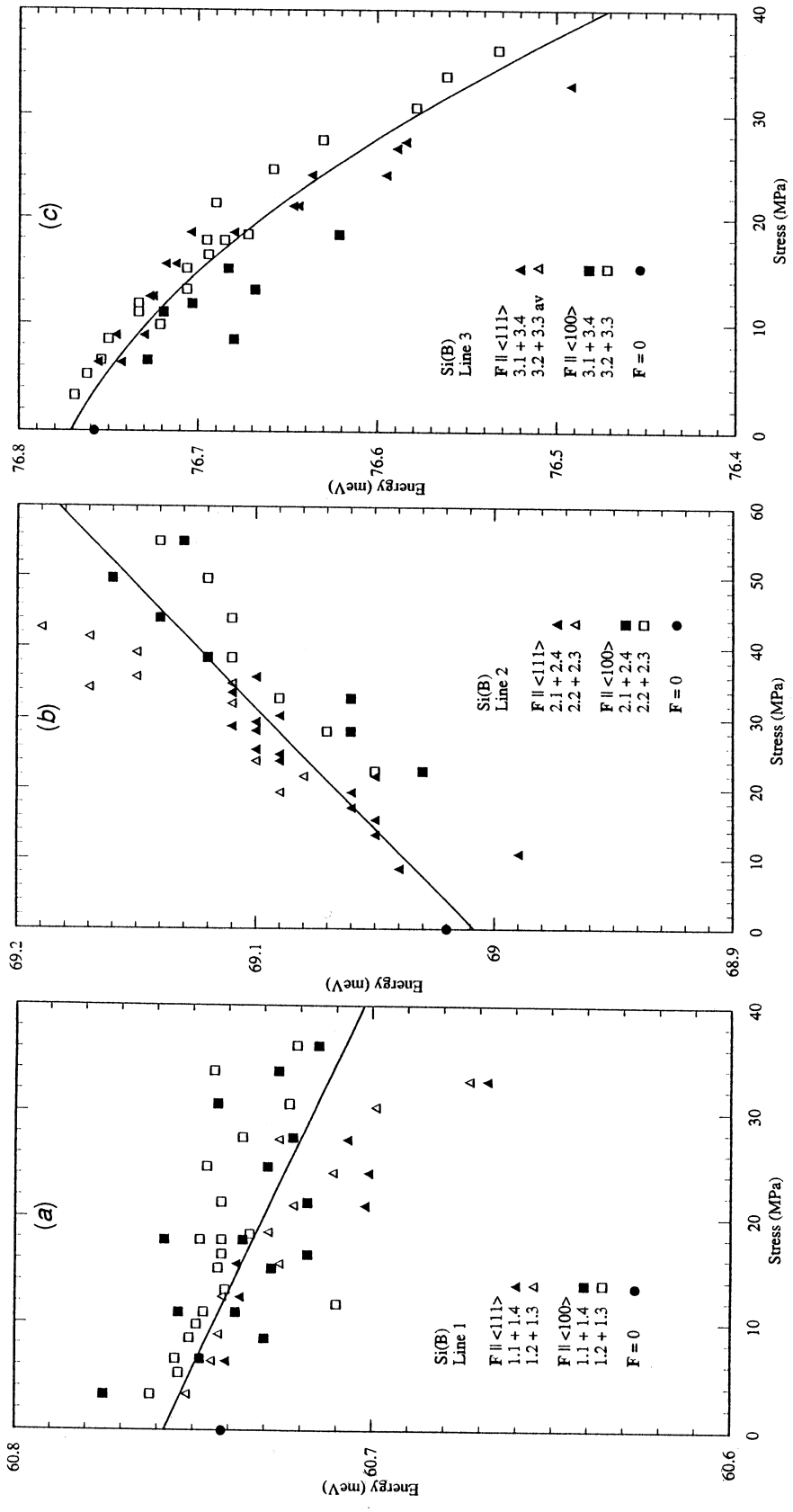
(a)
Si(B)
Line 1
F ∥ <111>
1.1 + 1.4
1.2 + 1.3
F ∥ <100>
1.1 + 1.4
1.2 + 1.3
F = 0
Energy (meV)
Stress (MPa)
(b)
Si(B)
Line 2
F ∥ <111>
2.1 + 2.4
2.2 + 2.3
F ∥ <100>
2.1 + 2.4
2.2 + 2.3
F = 0
Energy (meV)
Stress (MPa)
(c)
Si(B)
Line 3
F ∥ <111>
3.1 + 3.4
3.2 + 3.3 av
F ∥ <100>
3.1 + 3.4
3.2 + 3.3
F = 0
Energy (meV)
Stress (MPa)

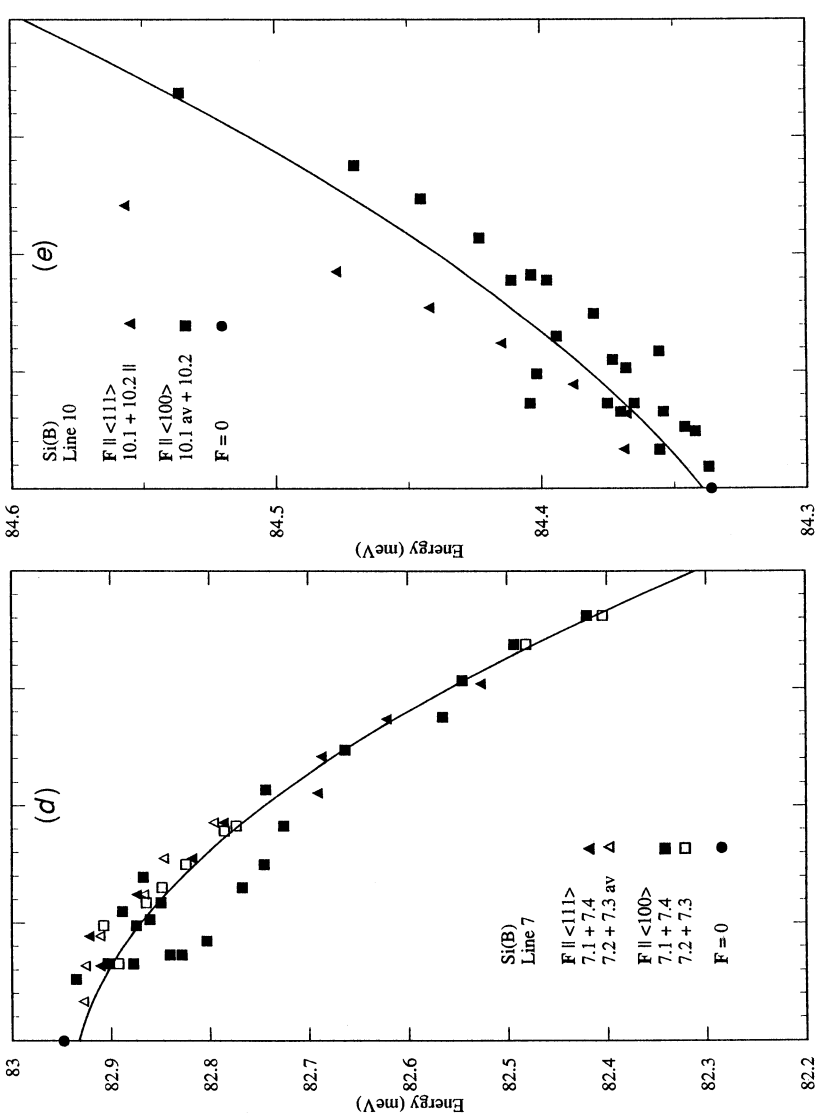

Fig. 14. (*a*) Stress dependence of the isotropic energy shift of the line 1 excited state relative to that of the ground state. (*b*) Stress dependence of the isotropic energy shift of the line 2 excited state relative to that of the ground state. (*c*) Stress dependence of the isotropic energy shift of the line 3 excited state relative to that of the ground state. (*d*) Stress dependence of the isotropic energy shift of the line 7 excited state relative to that of the ground state. (*e*) Stress dependence of the isotropic energy shift of the line 10 excited state relative to that of the ground state.

Data for $a_i - a_0$ for lines 1, 2, 3, 7 and 10 are given in Figs 14*a* to 14*e* respectively, and in Table 2. As might be expected the relative differences are small (of the order of 0·1 meV) over the range of stresses covered and generally increase with decreasing binding energy. No previous theoretical or experimental determinations of these deformation potential constants are known.

5. Conclusions

The spectrum of boron in silicon has been re-examined. Transition energies have been determined with a greater precision than previously and some new transitions have been identified. Excellent agreement with recent theory and previous experiment is obtained. Oscillator strengths and line widths have been measured for many lines, the former being in good agreement with theory. Spectra are shown in Figs 2 and 3 and the detailed data derived (as well as the experimental and theoretical results of others for comparison) are given in Table 1.

Piezospectroscopy has been performed using forces applied in the ⟨100⟩, ⟨110⟩ and ⟨111⟩ directions. Piezospectra, fan diagrams and energy splittings and shifts are shown in Figs 4 to 14, and the values of the deformation potential constants obtained are given in Table 2. The values of the ground state deformation potential constants b_0 and d_0 have been estimated using five spectral lines. The values are close to those given by Buczko (1987) and somewhat smaller in magnitude than those of Chandrasekhar *et al.* (1973). Excited state deformation potential constants b_i and d_i have been measured for lines 1, 2, 3 and 7 and are generally in agreement with the results of Buczko and smaller in magnitude than those of Chandrasekhar *et al.*, where these are given. It might be noted that the deformation potential constants for group III acceptors in germanium as calculated by Buczko (1987) are close to those observed experimentally (see Freeth *et al.* 1987). Relative isotropic deformation potential constants $a_i - a_0$ have been given for lines 1, 2, 3, 7 and 10.

Acknowledgments

The authors are grateful to: J. A. Campbell (University of Canterbury) and G. Piao for assistance with some of the measurements of line 2; C. A. Freeth and R. E. M. Vickers for the provision of computer source code adapted for data analysis and plotting; P. Ihnat for assistance in interfacing; and A. K. Ramdas (Purdue University) for provision of the silicon used in this work. This work was supported in part by the Australian Research Council and the University of Wollongong Board of Research and Postgraduate Studies.

References

Baldereschi, A., and Lipari, N. O. (1973). *Phys. Rev.* B **8**, 2697.

Baldereschi, A., and Lipari, N. O. (1974). *Phys. Rev.* B **9**, 1525.

Baldereschi, A., and Lipari, N. O. (1976). *In* 'Proc. 13th. Int. Conf. on the Physics of Semiconductors' (Ed. F. G. Fumi), pp. 595–8 (Tipografia Marves: Rome).

Bassani, F., Iadonisi, G., and Preziosi, B. (1974). *Rep. Prog. Phys.* **37**, 1099.

Beinikhes, I. L., and Kogan, Sh. M. (1988). *In* 'Shallow Impurities in Semiconductors 1988', Inst. Phys. Conf. Ser. No. 95 (Ed. B. Monemar), pp. 161–6 (Institute of Physics: Bristol and Philadelphia).

Beinikhes, I. L., Kogan, Sh. M., Novak, M. G., and Polupanov, A. F. (1990). *Mater. Sci. Forum* **65–6**, 259.
Beinikhes, I. L., Kogan, Sh. M., Polupanov, A. F., and Taskinboev, R. (1985). *Solid State Commun.* **53**, 1083.
Binggeli, N., and Baldereschi, A. (1988). *Solid State Commun.* **66**, 323.
Binggeli, N., and Baldereschi, A. (1989). personal communication.
Bir, G. L., Butikov, E. I., and Pikus, G. E. (1963). *J. Phys. Chem. Solids* **24**, 1467.
Bir, G. L., and Pikus, G. E. (1974). 'Symmetry and Strain-induced Effects in Semiconductors', pp. 438–43 (Wiley: New York).
Buczko, R. (1987). *Nuovo Cimento* **9D**, 669.
Buczko, R., and Bassani, F. (1988). *In* 'Shallow Impurities in Semiconductors 1988', Inst. Phys. Conf. Ser. No. 95 (Ed. B. Monemar), pp. 107–12 (Institute of Physics: Bristol and Philadelphia).
Buczko, R., and Bassani, F. (1989). personal communication.
Buczko, R., and Chroboczek, J. A. (1984). *Phil. Mag.* B **50**, 429.
Buczko, R., Blinowski, J., and Chroboczek, J. A. (1980). *J. Phys.* C **13**, 71.
Burstein, E., Oberly, J. J., Davisson, J. W., and Henvis, B. W. (1951). *Phys. Rev.* **82**, 764.
Chandrasekhar, H. R., Fisher, P., Ramdas, A. K., and Rodriguez, S. (1973). *Phys. Rev.* B **8**, 3836.
Chroboczek, J. A., Pollak, F. H., and Staunton, H. F. (1984). *Phil. Mag.* B **50**, 113.
Colbow, K. (1963). *Can. J. Phys.* **41**, 1801.
Cole, A. R. H. (1977). 'Tables of Wavenumbers for the Calibration of Infrared Spectrometers' (Pergamon: Oxford).
Cooke, R. A., Nicholas, R. J., Stradling, R. A., Portal, J. C., and Askenazy, S. (1978). *Solid State Commun.* **26**, 11.
Duff, K. J. (1993). *Phys. Rev.* B **48**, 5127.
Duff, K. J., Vickers, R. E. M., Fisher, P., Freeth, C. A., Takacs, G. J., Warner, A. D., and McLean, N. A. (1988). *In* 'Proc. 19th Int. Conf. Phys. of Semiconductors' (Ed. W. Zawadzki), pp. 1273–6 (Institute of Physics, Polish Academy of Sciences: Warsaw).
Fischer, D. W., and Rome, J. J. (1983). *Phys. Rev.* B **27**, 4826.
Fisher, P., and Ramdas, A. K. (1969). *In* 'Physics of the Solid State' (Ed. S. Balakrishna *et al.*), pp. 149–82 (Academic: New York).
Freeth, C. A., Fisher, P., and Simmonds, P. E. (1986). *Solid State Commun.* **60**, 175.
Freeth, C. A., Fisher, P., and Vickers, R. E. M. (1987). *In* 'Proc. 18th Int. Conf. on the Physics of Semiconductors' (Ed. O. Engström), pp. 841–4 (World Scientific: Singapore).
Guelachvili, G., and Rao, K. N. (1986). 'Handbook of Infrared Standards' (Academic: Orlando).
Hall, J. J. (1967). *Phys. Rev.* **161**, 756.
Hancock, R. D., and Edelman, S. (1956). *Rev. Sci. Instrum.* **27**, 1082.
Jagannath, C. (1980). Ph.D. Thesis (Purdue University).
Jagannath, C., Grabowski, Z. W., and Ramdas, A. K. (1981). *Phys. Rev.* B **23**, 2082.
Jagannath, C., and Ramdas, A. K. (1980). *J. Phys. Soc. Japan* **49**, *Suppl.* A201–4.
Kittel, C., and Mitchell, A. H. (1954). *Phys. Rev.* **96**, 1488.
Kogan, Sh. M., and Polupanov, A. F. (1978). *Solid State Commun.* **27**, 1281.
Lewis, R. A., Fisher, P., and McLean, N. A. (1988). *In* 'Shallow Impurities in Semiconductors 1988', Inst. Phys. Conf. Ser. No. 95 (Ed. B. Monemar), pp. 95–100 (Institute of Physics: Bristol and Philadelphia).
Lipari, N. O., and Baldereschi, A. (1978). *Solid State Commun.* **25**, 665.
Lipari, N. O., Baldereschi, A., and Thewalt, M. L. W. (1980). *Solid State Commun.* **33**, 277.
Loewenstein, E. V., Smith, D. R., and Morgan, R. L. (1973). *Appl. Optics* **12**, 398.
Luttinger, J. M., and Kohn, W. (1955). *Phys. Rev.* **97**, 869.
Merlet, F., Pajot, B., Arcas, Ph., and Jean-Louis, A. M. (1975). *Phys. Rev.* B **12**, 3297.
Onton, A., Fisher, P., and Ramdas, A. K. (1967). *Phys. Rev.* **163**, 686.
Pajot, B., Beinikhes, I. L., Kogan, Sh. M., Novak, M. G., Polupanov, A. F., and Song, C. (1992). *Semicond. Sci. Technol.* **7**, 1162.
Piao, G. (1992). Ph.D. Thesis (University of Wollongong).
Pikus, G. E., and Bir, G. L. (1959). *Fiz. Tverd. Tela* **1**, 1642.

Posener, D. W. (1959). *Aust. J. Phys.* **12**, 184.
Ramdas, A. K., and Rodriguez, S. (1981). *Rep. Prog. Phys.* **44**, 1297.
Rodriguez, S., Fisher, P., and Barra, F. (1972). *Phys. Rev.* B **5**, 2219.
Salib, E. H. (1982). Ph.D. Thesis (University of Wollongong).
Salib, E. H., Fisher, P., and Simmonds, P. E. (1985). *Phys. Rev.* B **32**, 2424.
Skolnick, M. S., Eaves, L., Stradling, R. A., Portal, J. C., and Askenazy, S. (1974). *Solid State Commun.* **15**, 1403.
Smakula, A., and Sils, V. (1955). *Phys. Rev.* **99**, 1744.
Swenson, C. A. (1983). *J. Phys. Chem. Ref. Data* **12**, 179.
Tekippe, V. J., Chandrasekhar, H. R., Fisher, P., and Ramdas, A. K. (1972). *Phys. Rev.* B **6**, 2348.
Vickers, R. E. M., Fisher, P., and Freeth, C. A. (1988). *Solid State Commun.* **65**, 271.
Wellman, P., Barlow, B. C., and Murray, A. S. (1985). Gravity base-station network values, Australia. Report 261 (Bureau of Mineral Resources, Geology and Geophysics: Canberra).
Yu, Z., Huang, Y. X., and Shen, S. C. (1989). *Phys. Rev.* B **39**, 6287.

Manuscript received 20 January, accepted 24 March 1994